Biofilm 3 (2021) 100057

Contents lists available at ScienceDirect

Biofilm

journal homepage: www.sciencedirect.com/journal/biofilm

Microbial fuel cells and their electrified biofilms

John Greenman [a], Iwona Gajda [a], Jiseon You [a], Buddhi Arjuna Mendis [a], Oluwatosin Obata [a,1], Grzegorz Pasternak [b,2], Ioannis Ieropoulos [a,*]

[a] Bristol BioEnergy Centre, BRL, University of the West of England, Frenchay Campus, BS16 1QY, UK
[b] Wroclaw University of Science and Technology, Poland

ARTICLE INFO

Keywords:
Electricity
Microbial fuel cell
Bioenergy
Perfusion electrodes
Synchrony

ABSTRACT

Bioelectrochemical systems (BES) represent a wide range of different biofilm-based bioreactors that includes microbial fuel cells (MFCs), microbial electrolysis cells (MECs) and microbial desalination cells (MDCs). The first described bioelectrical bioreactor is the Microbial Fuel Cell and with the exception of MDCs, it is the only type of BES that actually produces harvestable amounts of electricity, rather than requiring an electrical input to function. For these reasons, this review article, with previously unpublished supporting data, focusses primarily on MFCs. Of relevance is the architecture of these bioreactors, the type of membrane they employ (if any) for separating the chambers along with the size, as well as the geometry and material composition of the electrodes which support biofilms. Finally, the structure, properties and growth rate of the microbial biofilms colonising anodic electrodes, are of critical importance for rendering these devices, functional living 'engines' for a wide range of applications.

1. Introduction

The original example of all bioelectrochemical systems (BES) is the microbial fuel cell (MFC), first reported by Potter in 1911 [1]. MFCs (and MFC derived microbial desalination cells; MDC) are the only type of BES that produce electricity thanks to bioelectrochemical activity of bacteria forming a biofilm on the electrode surface. An MFC consists of two half-cells, i.e. the anode and cathode, usually separated by a semi-permeable membrane material. At initial sterile conditions, and for the same electrode material in both half-cells, there is no potential difference across the circuit. Following colonisation of one of the chambers by a bacterial community, that chamber becomes a negatively charged anode. The cathode usually consists of an oxidising agent (e.g. oxygen from free air), that completes the reaction, and closes the circuit. Closing the circuit, usually by applying an appropriate load resistor allows electrons to flow causing charge to be transferred, releasing the energy produced in the MFC.

The main components of the MFC are shown in Fig. 1a–e, illustrating examples of various designs and configurations. Microbes in the anode compartment are capable of utilising suitable organic substrates allowing them to grow and metabolise. This produces reducing power within the cell that can be tapped and transferred to the anode electrode by a number of mechanisms. These mechanisms are described in detail in Section 1.4.

1.1. Architecture of MFCs

MFC can be differentiated according to size: macro-, meso- or micro scale. One of the largest MFC systems to be reported is a modularised MFC with a total volume of 1000 L, operated successfully over 12 months [2]. This system did not consist of a single large MFC of 1000 L, but of 50 stacked MFC modules instead, each with a volume of 20 L. One of the smallest MFCs to be reported is a microfluidic 1.5 μL anode chamber with a 4 μL cathode chamber [3]. The largest (20 L) and the smallest (totalling 5.5 μL) give more than a 7-log fold difference in size. Therefore, scale and size of the anodic compartment is by far the biggest difference reported in MFCs and is therefore likely to have the largest effect on the formation and behaviour of the biofilms that colonise electrode surfaces. It appears that small scale MFCs (<20 ml) are more energy dense than larger volume systems [4,5]. Moreover, highest power outputs are thought to be maintained from the use of highly permeable, or perfusible electrodes [6]. What is lesser known is whether

* Corresponding author.
E-mail addresses: ioannis2.ieropoulos@uwe.ac.uk, ioannis.ieropoulos@brl.ac.uk (I. Ieropoulos).
[1] Currently at Newcastle University, UK.
[2] Currently at Wroclaw University of Science and Technology, Wroclaw, Poland.

https://doi.org/10.1016/j.biofilm.2021.100057
Received 15 April 2021; Received in revised form 29 July 2021; Accepted 19 August 2021
Available online 20 September 2021

or not MFCs containing diverse mixed communities can also show long term functional and ecological stability. This will be discussed in Section 3.3. However, microfluidic MFCs benefit from unique properties such as – laminar flow, surface tension, capillary forces, fluid-to-surface and fluid-to-fluid interfacial tension inherited from having microfluidic geometry [7]. The microfluidic scale further eliminates the external influence of inertial forces on the fluidic channel (Fig. 2). Microfluidic MFCs can also be membraned-based (M + MMFC) or membraneless (M−MMFC), however M−MMFC are more common in microfluidic scales, as laminar flow streams create separate layers in common channels. This feature eliminates the requirement for a physical membrane or separation for the anode and cathode. Construction examples range from traditional to photolithographic; photolithographic methods are common in sub-microlitre construction. Conductive polymers such as polyanilines (PANI) or polypyrrols (PPY) [8] in addition to graphene and traditional carbon materials employed in electrode construction can alleviate geometric constrains [9,10]. For a comprehensive review regarding microfluidic MFC, then readers are referred to Ref. [11].

The structure of the stereotypical MFCs as shown in Fig. 1 consists of two chambers separated by a membrane that allows ion exchange [12]. Membranes used for MFC architecture are expensive and prone to fouling, as well as present material integrity challenges in long term use. To overcome the drawbacks of commercial membranes, alternative materials have been investigated as MFC separators. Ceramics such as earthenware, terracotta or clayware are some of the most commonly used because of their low cost, natural availability, robustness for long-term processes and their low maintenance requirements that facilitates their use in commercial applications [13] (Fig. 3). On the contrary, polymeric proton exchange membrane (PEM) have the obvious disadvantage that they are not recyclable, and the material is chemically inert and slow to break down or biodegrade in the environment [14]. Furthermore, they are relatively expensive compared to ceramic membranes [15].

There are of course those MFC architectures that are truly membraneless, in the sense that there is no separating material between the anode and cathode electrodes. Instead, polarity difference occurs due to redox gradients that are the result of heterogeneous conditions; the classic example describing this is the Winogradsky column and heterogenous conditions are achieved when the cathode electrode is partially in the bulk and partially exposed to air [16,17]. Potential applications include *in situ* maritime/environmental and weather telemetry instruments [18,19]. This is a well-covered topic and so will not be extensively discussed here.

A highly diverse range of microorganisms have been found to be capable of forming biofilms on electrodes, both anodes and cathodes. Species that interact with the anode have been referred to as anodophiles [20], exoelectrogens [21], electricigens [22], electrochemically active microorganisms [23], anode-respiring [24] or electrogenic [25]. Whether or not this terminology accurately describes the real purpose of these microbes in natural ecosystems is open to debate but for the purposes of this discussion, it would suffice to say that in MFCs, the generated power is a direct function of microbial colonisation.

1.2. Mechanisms of electron transfer

1.2.1. Synthetic (exogenous) mediators

Allen and Bennetto were the first researchers to utilise synthetic soluble redox mediators as a means to harvesting the reducing power of living bacteria [26]. It should be noted that any microbial cell within the anodic chamber, whether attached to the electrode or in planktonic suspension may contribute to power generation providing it is permeable to the mediator molecules. One of the earliest mediators used was the redox dye methylene blue, first prepared in 1876 by the German chemist Heinrich Caro [27]. According to Arup [28], it was Neisser and Wechsberg in 1900, who first suggested that methylene blue was a useful medium for judging the bacterial contents of milk. Soon after, the

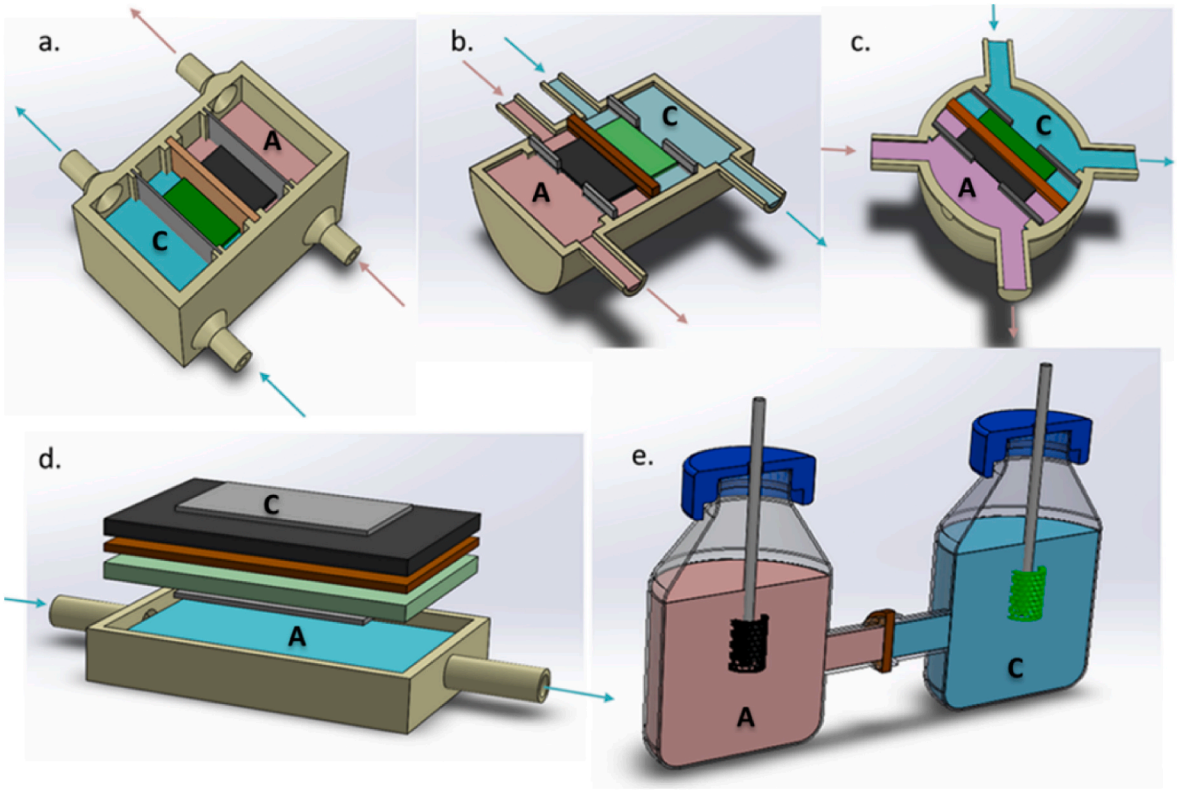

Fig. 1. Examples of membrane-based MFC designs: a) cuboid, double chamber MFC, b) cylindrical double chamber MFC, c) spherical double chamber MFC, d) cuboid MFC with open to air cathode, e) H-type, double chamber MFC. In all designs, "A" and "C" indicate anode and cathode respectively. Inputs and outputs (when these are used for continuous flow) are marked with arrows.

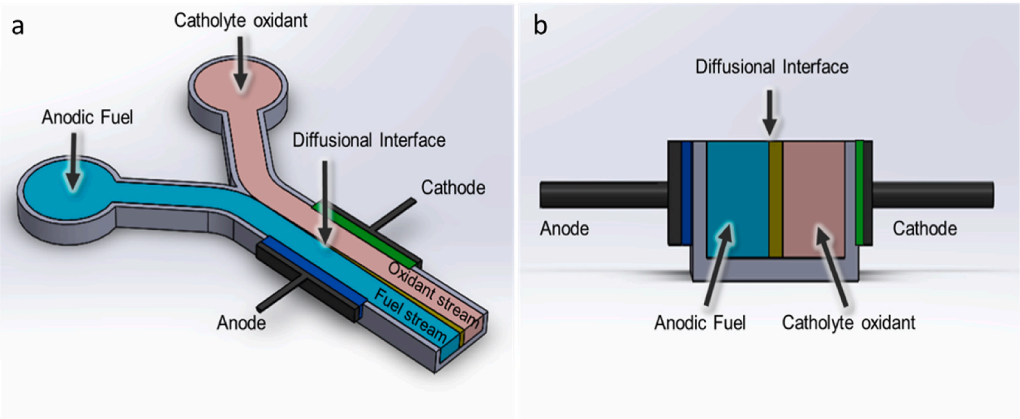

Fig. 2. Schematic design of M-MFC: a) top view, b) cross section.

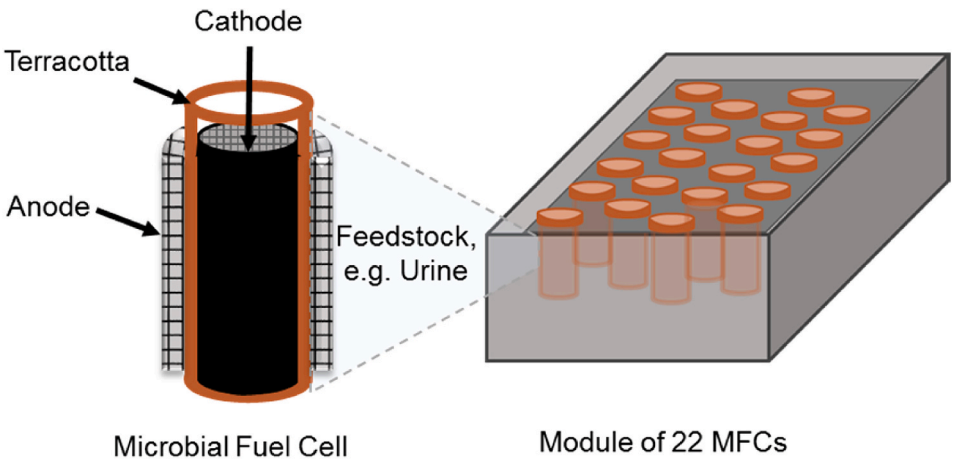

Fig. 3. Non-polymeric membranes e.g. terracotta MFC with a multi-MFC modular stack.

methylene blue reduction test was used in the field of dairy manufacturing. The test was based on the fact that the blue colour imparted to milk by the addition of methylene blue, disappears depending on a number of factors, most important of which are the bacterial content of the milk, its growth rate and the operating temperature. If all controlling factors are kept constant other than the bacterial content of the milk, the time required for the colour to disappear will be determined by the number of bacteria. Some of the best artificial mediators known for use in MFCs, in addition to methylene blue are: thionin, neutral red, 2,6-dichlorophenol, indophenol, safranine-O, phenothiazine, and benzyl viologen [29,30] (Fig. 4a).

1.2.2. *Natural (endogenous) mediators*

Habermann and Pommer [31] described MFCs that used sulphate reducing bacteria (SRB) to generate hydrogen sulphide that was active at the anode, being oxidised back to sulphate (or other oxyanions of sulphur). *Shewanella oneidensis* MR-1 secretes flavins (FMN, FAD and riboflavin) in the concentration range of 100–500 nM after 1 week of operation [32], while phenazines, are also excreted by *Pseudomonas aeruginosa* [33]. With the exception of SRB that can reduce sulphate to sulphide as an important part of their central metabolism, the production rate of soluble mediators like FMN and FAD is likely to be slow and they may only produce significant concentrations in batch culture in the stationary phase when many cells are lysing or if the anode environment is poised at the redox level, which is suitable for accelerated mediator generation [34] (Fig. 4a).

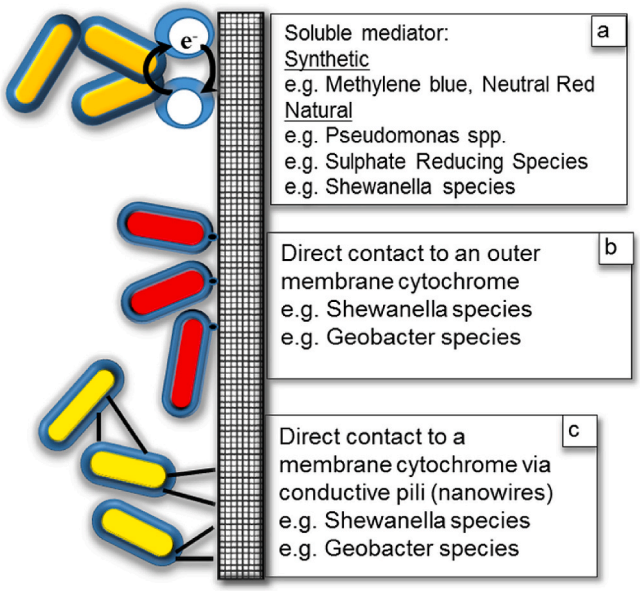

Fig. 4. Three main mechanisms for anodic electron transfer from cell reducing power (NADH/NADPH) to the anode electrode in MFC through (a) soluble mediator, (b) direct contact to an outer membrane cytochrome, (c) direct contact to a membrane cytochrome via conductive pili.

1.2.3. Direct electron transfer

Up until now, only a few genera and species have been shown to be electrochemically active by means of direct conductive mechanisms; these include *Shewanella*, *Geobacter, Rhodoferax ferrireducens, Pelotomaculum thermopropionicum, Geothrix and Geoalkalibacter*. Of these, *Geobacter* and *Shewanella* have been studied the most. The first group to report this phenomenon were using *Shewanella* [35], that was later named as a cable bacterium [36]. A summary of important components in the electron transport mechanism from cells to the anode in *Geobacter* MFCs has been provided by Lovley [37]. Metabolism of electron rich (reduced) substrate such as acetate or lactate drives the production of reduced NADH from NAD^+ within the cell. In order for the cell to maintain reducing power, it must re-oxidise NAD^+ by abstracting electrons by using dehydrogenase and the cytochrome system consisting of quinone/menaquinone pool, periplasmic proteins MacA, PpcA, and outer membrane proteins, OmcE and OmcS. Together these are able to transport the electrons by a series of redox reactions spanning the inner cytoplasmic membrane across the periplasmic space until the electron is conducted across the outer membrane to the anode electrode via the outer membrane cytochromes OmcE and OmcS (Fig. 4b). Further transfer of electrons, even within multilayers of cells may also occur, via a dense network of appendages with metal-like conductivity called bacterial nanowires [36]. The transfer may occur cell by cell over distances of more than 1 cm, until electrons are donated to the electrodes [38] (Fig. 4c).

Comparison of the electrode respiring capacity of wild type *Shewanella decolorationis* S12 and an outer membrane cytochrome-C (OMC)-deficient mutant [39] showed that the mutant had a much-reduced capacity at producing current, but not zero, probably due to the secretion of flavin molecules, suggesting that some species may use all three transport mechanisms shown in Fig. 4. The majority of species studied to date are Gram negative organisms. However, *Thermincola potens* strain JR, is a Gram-positive isolate obtained from the anode surface of a microbial fuel cell [40]. Despite careful study this species produced no evidence of any soluble redox-active components being secreted into the surrounding medium. Confocal microscopy revealed highly stratified biofilms in which the cells contacting the electrode surface were disproportionately viable relative to the rest of the biofilm. Furthermore, there was no correlation between biofilm thickness and power production, suggesting that cells in contact with the electrode were primarily

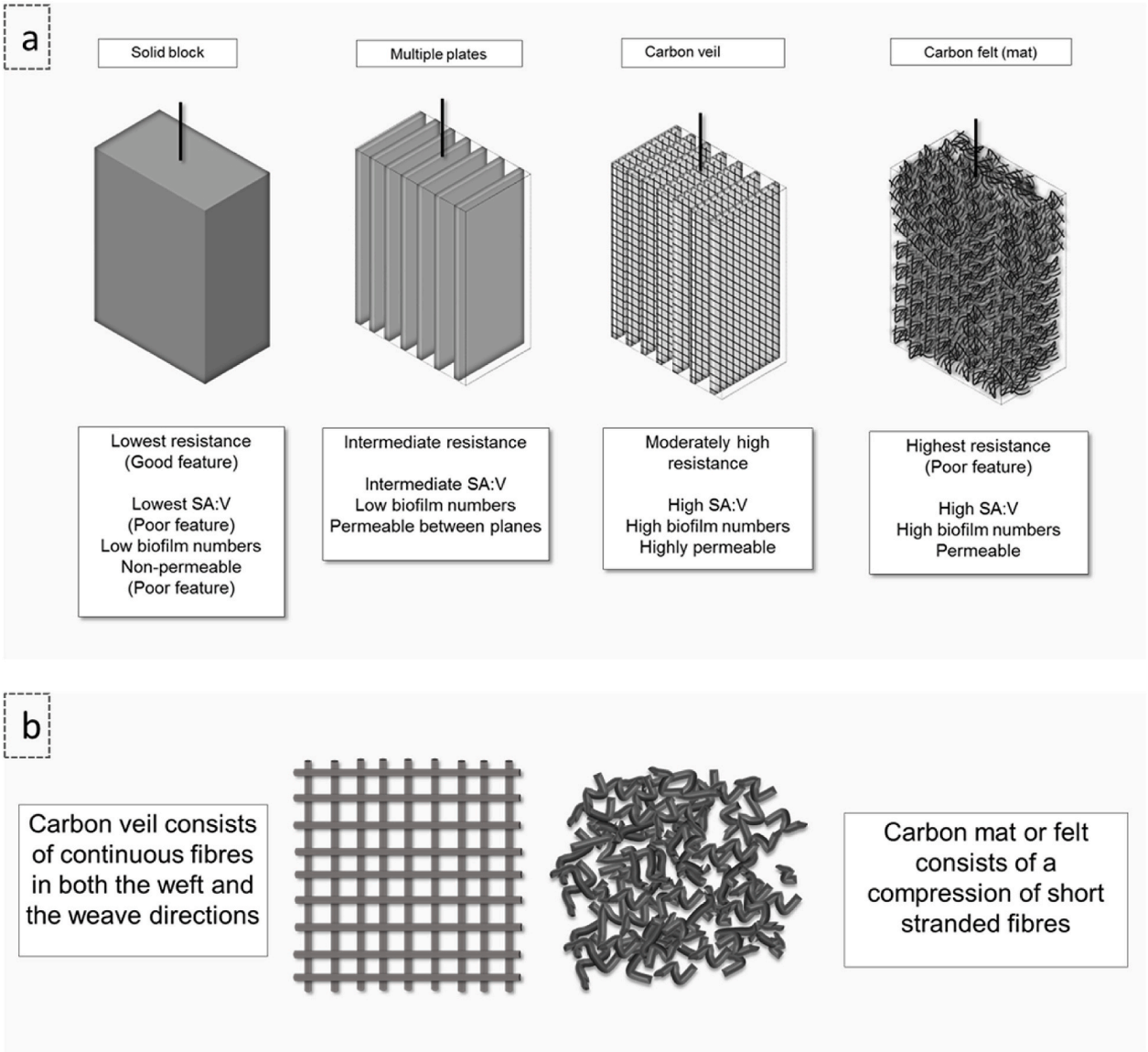

Fig. 5. MFC carbon electrode structure: a) plain carbon electrodes of same geometric macro size compared and b) carbon veil and carbon felt (or mat) compared. SA: V represents the surface area to volume ratio.

responsible for current generation.

1.3. Electrodes

In general, the higher the macro-scale (geometric) surface area of electrode (Fig. 5a), the higher the potential area for accommodating a microbial colony, that would potentially result in higher power output. However, felt, veil or foam electrode materials possess both micro and nano-scale geometries, including pores. Research shows that power output is both electrode area and pore diameter dependent [41,42] and in the case of *Shewannella*, power is optimal at 5~7 μm of biofilm thickness [41]. Recent research shows that controlled micro and nano porous configurations increased current density [43]. Electrode materials and geometry differ depending on MFC volume; common materials include carbon, carbon composites and mixtures in the form of blocks, rods, brushes, felt, cloth and veil. In constructing microscale electrodes, metal or carbon conductive material is coated thinly by placement or deposition to give a large surface area [44]. In larger scale electrodes, the use of carbon veil as electrode material proves advantageous due to (i) sufficient microchannels, that allow high permeability enabling nutrient transfer through advective transport via perfusion; (ii) thread continuity, that results in low resistance in comparison to carbon felt or other carbon material discontinuity of strands (Fig. 5b).

2. Biofilms

The widely believed conception or hypothesis could be reasonably called the conventional biofilm paradigm (Fig. 6). The challenge with paradigms is that they get taken for granted, without subsequent critique. The following description and history of biofilms follows a common start for all theories of biofilm formation but then moves toward an alternative view of what is commonly accepted.

Formation of a thick (diffusion-limiting) biofilm attached to an impermeable substratum (e.g. graphite block). This is the conventional paradigm. Biofilms thicker than 20–50 μm are most likely to be diffusion limiting and stratified. Feedstock substrates diffuse into the biofilm but outer layers of cells will utilise the substrate leaving less for the inner layers. This gives rise to the formation of gradients for both the end terminal electron acceptors (e.g. oxygen) and carbon-energy (C/E) substrates. Both gradients go from the outside to the inside. In addition, the biofilm matrix fluid has a long replacement time and the mean growth rate of the total biofilm is slow. Inner cells may be close to starvation and trying to survive rather than grow. This gives rise to erosion due to layers of inactive cells whilst cells in the outer layers grow fast. It is probable that aerobes have majority towards the outside whilst anaerobes have majority deep inside with facultative species being distributed throughout (i.e. showing ecological stratification).

2.1. Biofilm history

Over 300 years ago, Antony van Leeuwenhoek reported to the royal Society of London [45] that he had observed a vast accumulation of microorganisms in dental plaque using microscopy. He stated, "the number of these animalcules in the scurf of a man's teeth are so many that I believe they exceed the number of men in a kingdom." Early work showing that microbes can adhere and grow on wet surfaces when exposed to nutrients was noted in the 1930s, by Henrici [46] and Zobell and Allen [47]. Their experimental devices consisted of microscope slides in special holders. They submerged the slides for varying lengths of time before retrieving them and analysing the attached growths microscopically. In 1940, Heukelekian & Heller [48] conducted experiments using *E. coli* and glass beads in small bottles with dilute nutrients (tryptone and glucose) and concluded that "Surfaces enable bacteria to develop in substrates otherwise too dilute for growth. Development takes place either as bacterial slime or colonial growth attached to other surfaces. Once a biologically active slime is established on surfaces, the rate of biological reaction is greatly accelerated". Jones et al. [49] were the first to use scanning and transmission electron microscopy to examine biofilms on trickling filters in a wastewater treatment plant and showed them to be composed of a variety of organisms (based on cell morphology). Moreover, these researchers were also able to show that by using ruthenium red stain coupled with osmium tetroxide fixative,

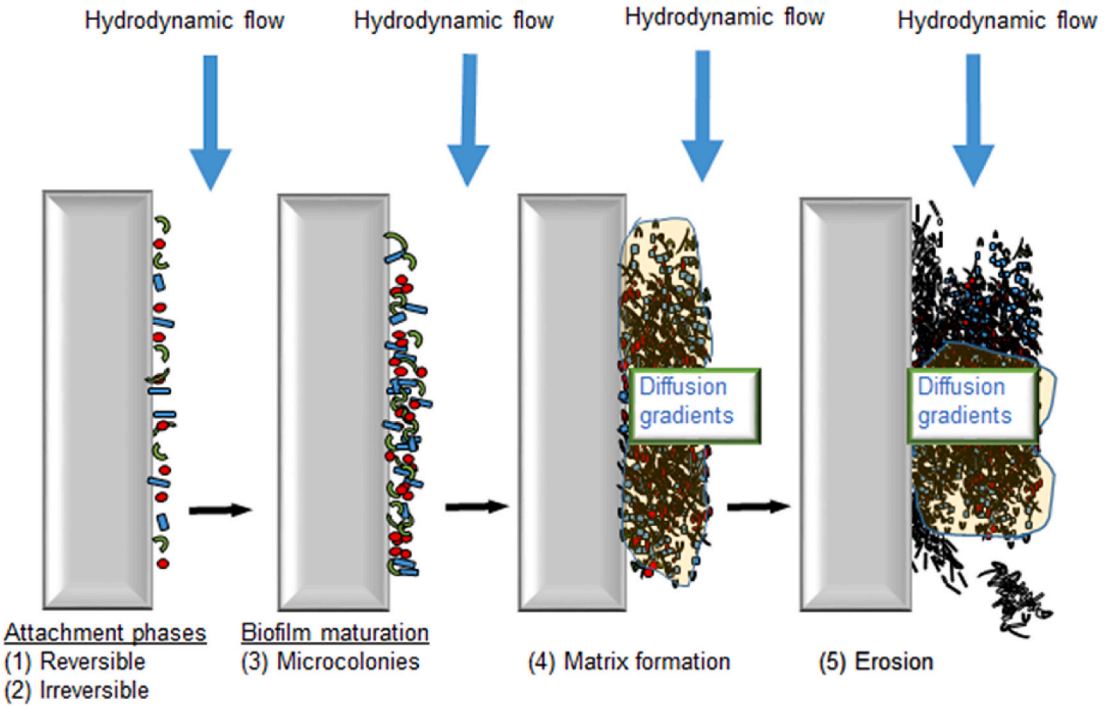

Fig. 6. Conventional biofilm paradigm indicating the attachment phase (1) and (2), biofilm maturation forming microcolonies (3), then matrix formation (4) and erosion (5).

the matrix material surrounding and enclosing cells in observed biofilms was mainly polysaccharide based. Characklis [50] studied microbial slimes in industrial water systems and showed that they were not only very tenacious but also highly resistant to disinfectants such as chlorine. In 1978, Costerton et al. [51] put forward a theory of biofilms explaining the mechanisms whereby microorganisms adhere to living and non-living materials and the benefits accrued by this ecological niche. Although Zobell and Allen [47] used the term "bacterial film" it was Mack et al. [52] who first used the term biofilm. In the medical-dental field the term was first used by Jendresen and Glantz [53] and Jendresen et al. [54], and in the same year it was first used in the field of microbiology by Costerton [55]. Since then, the biofilm based research grew in importance, both in the medical and environmental fields developing and perfecting the methodology of investigation.

2.2. Biofilm (physical) models

The most common technique for producing biofilms for research purposes, is by use of a microtiter array of periodically fed biofilms in small plastic wells [56] inoculated with target organisms and incubated to form biofilms. Following incubation, planktonic bacteria are rinsed away, and the remaining adherent bacteria (biofilms) are stained with various vital stains (e.g. crystal violet), that allows for the visualization and quantification of the biofilm. The main advantages include the provision of having many replicate wells for either test or control conditions giving data with high levels of statistical confidence. However, multi-well biofilm systems do not possess longevity, and the batch or fed batch system cannot allow cells to reach steady state conditions compared to models having a continuous flow stream. The first description of a continuous flow system was reported by Russell and Coulter [57] using an artificial mouth apparatus. This consisted of a vessel with an input delivery port allowing nutrient solutions (artificial saliva) to be drip-fed on to a real or artificial tooth surface as the biofilm substratum. The outflow was removed to a waste bottle. Another specially designed biofilm apparatus included an open system model [58,59] that used a continuous flow system combined with a mechanism to ensure that the biofilm remained at a constant thickness. This system was called the constant depth film fermenter (CDFF). Other devices for producing biofilms included the Robbins device [60] and the Calgary device [61]. All these systems allowed for many replicate biofilms to be produced with high reproducibility for samples taken from the same vessel over time. However, none of these systems allowed for accurate biofilm growth rates to be determined or controlled and the growth rates of the biofilm cells were left ill defined. Two conflating parameters contribute to the growth of the biofilms; growth from attached cells within and further attachment of cells from without. None of the above models are able to separate the contributions made from these two adherence parameters.

A separate methodology invented at an earlier period by Helmstetter and Cummings [62] described what has since been called a "baby factory" for microbes. In this system a population of cells were deposited and trapped on the uppermost side of paper or polymeric microporous membrane. The membrane was then inverted, and sterile culture medium was continuously supplied by allowing it to flow through the membrane. The attached cells grew, but the force of the medium flow removed all the new progeny (described as "daughter cells") that was predominately unattached. The Perfused Biofilm Fermenter (PBF) [63] also consists of a membrane to which a population of bacteria are attached through filtration. The membrane is then inverted and perfused with culture medium. The same idea was continued by Gander & Gilbert [64] using cellulose nitrate Swinnex filters. Cells, pressure filtered on to membranes *in situ*, were perfused from the sterile side and the cells observed to grow. The growth rate of the attached cells was shown to be proportional to the flow rate of medium and steady-state conditions were attained for a number of days. Hodgson et al. [65] used a perfusion model based on Sorbarod filters (a cylindrical bundle of cellulosic strands). This method was favoured because it has a substratum surface many times greater than the membrane filters, supporting a much higher number of attached cells than controls not using the Sorbarod matrix [64]. This system was also capable of supporting the growth of the biofilms for periods of several days. A similar system [66], has been described using a small 1 cm^3 block of cellulose matrix fed from above by drops of growth medium. This was termed a perfusible flat-bed model. Many other groups of researchers have used the same or very similar perfusion models [67]. A recent variation of the flat bed model includes the use of a three-dimensional collagen gel matrix comprised of a mesh of polymerized type I collagen fibres to simulate the semi-solid wound environment found in vivo [68]. Many perfusion models can be enhanced by combination with real time sensors such as pH microelectrodes [69] or systems to measure and monitor volatile organic compounds (VOCs) for example using SIFT-MS [68]. Most perfusion systems show steady state by 24–48 hours which may continue up to the end of the reported experimental time period of 96 hours [70]. Of interest in this review is the similarity of a cellulosic matrix to that produced by folding carbon veil material into an electrode to form the anode of an MFC. This idea was tested by Ledezma et al. [71] using the electrogenic species *Shewanella oneidensis* strain MR-1 and revealed that, like other perfusion systems, the biofilm growth rates can be controlled by the operator by changing the flow rate of C/E limiting medium.

In 2015, Helmstetter [72] summarised the background story to the development of the "baby machine" technique with the main interest to understand the basic bacterial division cycle. The original intention was to seek a method to produce synchronous growth with minimal disturbance; not to prolong the growth of the attached biofilm cells. It is interesting to note that all perfusion biofilms that reach steady state growth will be growing asynchronously, but any detached daughter cells taken at any particular time point should be in synchronous growth since the released cells are all bound to be at about the same point in their respective growth cycle (i.e. just after septum formation and breaking away from the mother layer). If synchrony is achieved the outgrowth of the incubated planktonic sample will show a characteristic step pattern as all cells divide at about the same time.

2.3. Biofilm attachment and detachment processes

When sterile surfaces are exposed to an aqueous medium containing proteins and charged polymers (not cells) they are rapidly adsorbed on to the surface. This adsorption occurs within seconds. The conditioned surfaces may probably influence the types of bacterial species that may colonise the surface thereafter. Surface conditioning occurs in seawater [73] and on salivary exposed tooth enamel surfaces in the mouth [74].

The initial attachment of cells to a solid substratum is governed by forces including advective flow, and three types of non-covalent forces (1) Lifshitz–van der Waals (LW) or electrodynamic interactions, (2) Lewis acid-base (AB) and (3) electrical double layer (EL). All these interactions are considered in the extended DLVO (XDLVO, DLVO stands for Derjaguin, Landau, Verwey, Overbeek) theory [75,76]. The free energies for each type of interaction as a function of distance can be determined and treated separately and then all three (expressed in the same energy units) may be added together, to obtain the final XDLVO plot. Other factors that could have effects on initial binding include divalent metal ions (Mg^{2+} and Ca^{2+}) that form ionic bridges between negatively charged molecules or particles. Additional forces include the motility of cells by flagella that may drive cells in directions along concentration gradients (chemotaxis), across or towards electric fields (electro and Galvano-taxis), magnetic fields (magnetotaxis) and towards light (phototaxis) [77]. For mixed species communities, once pioneer species have bound to a substratum, they increase the diversity of binding sites for secondary colonisers. Specific mechanisms for co-colonisation include early colonisers of the tooth surface that specifically bind and co-aggregate with pioneer and secondary colonisers [78]. For example, a lectin ligand on one cell species can interact with a

complementary lock and key glycoprotein receptor on the other species. Such coaggregation offers an explanation for the build-up of dental plaque in the human mouth but appears to be equally important for environmental biofilms [79,80].

There are many interacting variables thought to be important in cell attachment and biofilm formation [81]. These include the types of substratum, their texture, roughness and hydrophobicity. The conditioning layer may also be important. The cell surface properties include, flagella, pili, fimbriae, capsules and/or slime formation (extracellular polymeric substances) and the physicochemical properties of the bulk fluid feedstock. The latter includes nutrient types and concentrations, pH, redox, presence of divalent metal ions, oxygen, inhibitory compounds and temperature.

In the biofilm detachment process, distinct mechanisms include erosion and shearing where there is continuous removal of small clumpy portions of the biofilm; sloughing (rapid and massive removal), abrasion (detachment due to collision of particles from the bulk fluid bombarding the biofilm surface) and natural shedding. These models of dispersal may affect the phenotypic characteristics of the organisms. Eroded or sloughed aggregates from the biofilm are most commonly observed with thicker biofilms that develop in nutrient-rich environments [82]. The aggregates are likely to retain certain biofilm characteristics, such as extracellular polymeric substances (EPS), antimicrobial resistance properties, whereas cells that have been shed as a result of growth (i.e. natural single cell separation) may revert quickly to the planktonic phenotype. As expected, the rate of erosion from the biofilm increases with increases in biofilm thickness along with high fluid shear at the biofilm-bulk liquid interface. Sloughing is more random than erosion and is thought to result from nutrient or oxygen depletion within the biofilm structure [83]. At high hydrodynamic shear rates, hard mineral particles in the input medium may remove biofilms by abrasion.

The natural process of shedding is an important process for small scale MFC bioreactor with perfusible anodes (Fig. 7). The mechanisms underlying the shedding process require actively growing cells to separate soon after the formation of a distinct cell wall septum between actively dividing cells, as a trigger to total separation between them. In the thick film paradigm, most cells remain stuck and impacted in EPS and only detach in large clumps. For perfusible anodes at high flow rate with thin films there is a monolayer theory whereby the monolayer is fixed in location with high adhesion for many years and may be called the inner core "mother layer" and that all new cell biomass is naturally shed into the planktonic phase in the form of daughter cells. This assumes that the electrode is saturated with regard to binding receptors for new cells so that biomass accumulation by the electrode as a whole is zero. Before the advent of the MFC methods for studying fixing biofilms included membrane elution techniques used for obtaining division synchrony [62]. These researchers showed that loosely bound cells following inoculation are rapidly displaced from the membranes with flow rate and that the remaining attached cells grow and achieve steady states by shedding off daughter cells that divide synchronously on subsequent transfer to fresh media. Experiments using Sorbarods and/or small cellulosic perfusible matrices [66] have shown steady state stability for a few weeks, however MFCs may remain stable for many years. Gilbert et al. [84] considered cell surface hydrophobicity to be an important feature of biofilm dispersal, where the hydrophobic character of the newly divided daughter cells eluted spontaneously from the biofilms with the spent medium. This was unaffected by the growth rate of the parent culture and was more connected with cell division rather than growth rate, per se. It has also been shown that the electrophoretic mobility properties changed [84] as a function of their division cycle, as did the non-specific adhesion to glass slides, suggesting that the cells dispersed from the biofilms were relatively "unsticky" [85], but became "sticky" again upon continued incubation and growth.

2.4. Diverse mixed cultures and exoelectrogens

All life-forms on the planet have been categorised into one of three domains, Bacteria, Archaea and Eukarya. Microorganisms in MFCs tend to fall into the categories of Bacteria and Archaea, although yeasts (Eukarya) can often be isolated from highly diverse communities. The bacteria that have been isolated fall into many sub-categories including (in alphabetical order): Acidobacteria, Actinobacteria, Aquificae, Bacteroidetes/Chlorobi group, Chloroflexi, Cyanobacteria, Firmicutes (Gram positive), Nitrospirae, Planctomycetes and Proteobacteria of which there are four groups (Alpha, Beta, Gamma and Delta/Epsilon). The phyla continue with Spirochaetes, Thermotogae and

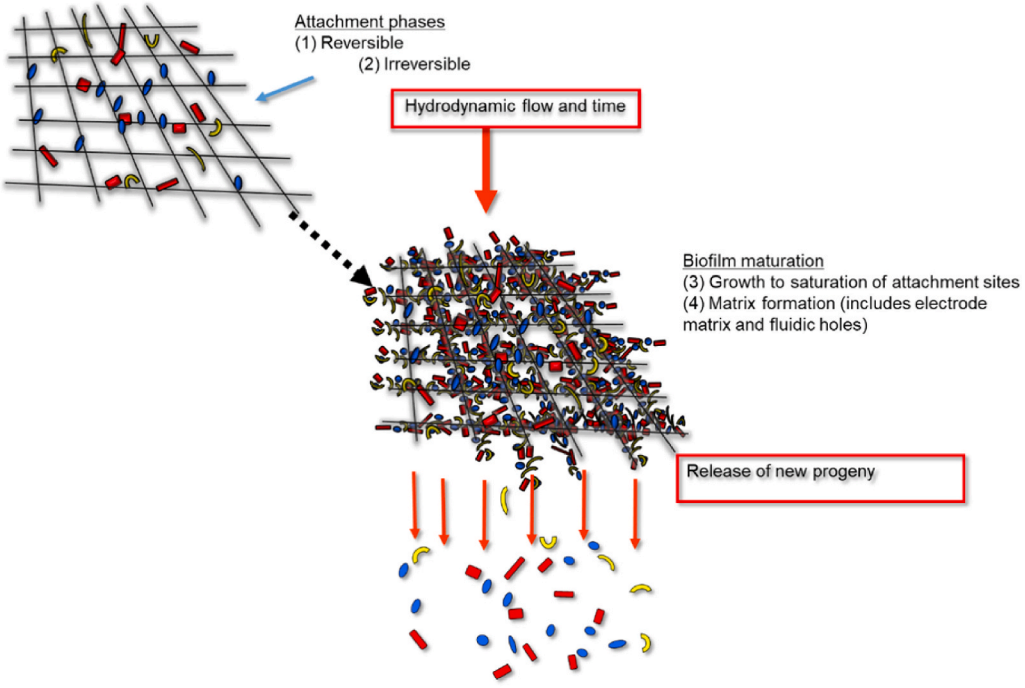

Fig. 7. Alternative biofilm theory for perfusion biofilms and carbon veil electrodes illustrating process of attachment, colonisation and maturity.

Thermotogales. Species that are thought to be electrogenic can be found from many of the above phyla. A review by Zhang, Jiang and Liu Y [86] suggested the following species (among others) were electrochemically active at the anode: Alpha-Proteobacteria included *Ochrobactrum anthropic*, *Rhodopseudomonas palustris*, *Rhodobacter sphaeroides* and *Acidiphilium cryptum*. The Beta-Proteobacteria included *Rhodoferax ferrireducens*, whilst the Gamma-Proteobacteria included *Shewanella putrefactions* and *Shewanella oneidensis*. The Delta-Proteobacteria include *Geobacter metallireducens* and *Geobacter sulfurreducens*. The Epsilon-Proteobacteria include *Arcobacter butzleri*, whilst the Firmicutes included *Clostridium butyricum* and *Clostridium beijerinckii*.

A semi-quantitative abundance analysis of wastewater treatment MFC [87] indicated a very wide diversity of species. The MFC was operated over 300 days in repeat-batch mode where the solution was replaced every 2 weeks with primary effluent. The phylogenetic analyses of anode-associated electricity-generating biofilms showed that the microbial populations temporally fluctuated and maintained a high biodiversity throughout the year-long experiment. Abundant phylotypes isolated from the electricity generating consortia from the anodic biofilm included Deltaproteobacteria (e.g. *Geobacter* species), but also species closely related to *Desulfuromonas acetexigens*. From the Epsilonproteobacteria, phylotypes closely related to *Arcobacter cryaerophilus* were only found in the early stages of anode community development but were abundant in the primary effluent, suggesting that the bacterium was simply introduced from the wastewater but did not thrive at the anode surface during prolonged electricity generating conditions. The phylum Bacteroidetes was also abundant in the anode biofilm and various abundant phylotypes were observed throughout the long-term MFC operation and phylotypes found in the anode-associated consortia were not observed in the raw primary clarifier effluent.

2.5. Detachment of exoelectrogens and other biofilm species

There are important differences between biofilms forming on impermeable substrata (e.g. graphite block electrode) and biofilms that form on a permeable (perfusible) substratum (e.g. carbon veil electrode). The most important difference is the supply and distribution of available nutrients from the feedstock to bacterial cells as well as the biofilm architecture. At the macro and meso scale, on the impermeable surface, the biofilm forms a matrix that does not include the substratum that is a separate and distinct compartment. For a biofilm forming on impermeable carbon blocks, what forms at meso-microscale is the interpenetration of substratum and voids of liquid. Nutrient substrates are supplied by advective transport of molecules; there is next to zero diffusion limitation. The biofilm that forms on the graphite block will probably grow into a thick biofilm. Under conditions of batch culture or very slow flow rate chemical gradients will form, slowing the growth rates of the innermost layers. Colonisation of an anode electrode of *Geobacter sulfurreducens* was studied by Bond and Lovley [88], using SEM that revealed nearly full coverage of the entire electrode surface by a thin layer of cells, rarely more than a few cells thick.

In another study of colonisation by Read et al. [89] biofilms were allowed to form with pure culture Gram-negative and Gram-positive species. When the anode was in open circuit the viability of the cells was highest on top of the biofilm, furthest away from the anode. However, for electrodes connected by an electrical load, the viability remained high for all cells nearest to or touching the electrode while cells became non-viable on top or further away from the electrode. This showed that current flow might well make a difference in shaping the colonisation phase. A study showed that *Geobacter sulfurreducens* biofilms with a thickness of ~20 μm was more electrochemically active than thicker biofilms greater than 45 μm [90]. This indicates that high diffusive resistance is occurring because of slowness in the rate of substrate transfer from their source (in the medium) into the inner layers or core of the biofilm with physical contact with its end-terminal electron acceptor. Too much accumulation on the electrode will weaken power density of the MFC.

To study this phenomena, electrodes and real time optical microscopy were used by McLean et al. [91] to determine the effect of low populations of *Shewanella oneidensis* strain MR-1 when under external resistance of 1MΩ a thick mature biofilm was formed with tower morphology (>50 μm thick) and low power output. In contrast, the anode with the heaviest load (100 Ω) gave the thinnest biofilms (<5 μm thick) yet were more powerful. Xiao et al. [92] showed that *Shewanella oneidensis* MR-1 cells containing extracellular polymeric substances (EPS) could be treated by washing in reagents that removed the EPS components without damaging the viability of the cell. The authors noted that such prepared EPS-depleted MR-1 gave maximum current increments of between 40 and 90% higher than that of the control group of MR-1 cells producing EPS. They concluded that MR-1 in the presence of EPS was less efficient at transporting electrons than biofilms without EPS. Pasternak et al. [93] using a highly diverse mixed culture MFC observed the same phenomena that a low resistance load, gave thinner biofilms with higher power output than electrodes exposed to high external resistance load, which gave thick biofilms but with low power output. With regard to the attachment and detachment processes, then Thormann [94] noted that *Shewanella* biofilms could change the state from attachment to detachment and that cyclic di-GMP was a key intracellular regulator for this process. Zhou et al. [95] also using *Shewanella oneidensis* identified three important genes, coding for a biofilm-promoting protein (BpfA), a periplasmic transglutaminase-like cysteine proteinase (BpfG) and a bifunctional diguanylate cyclase/-phosphodiesterase (BpfD). These genes were responsible for the regulation of biofilm formation and detachment in *Shewanella oneidensis* biofilm grown on plastic surfaces. In small-scale MFC, all the detachment behaviour of the biofilm will be aided by the magnitude of the substrate flow rate as laminar flow through the anodic volume that exert a shear force that can help the detachment process by removing weakly attached cells into the planktonic flow. It is assumed that the forces of adhesion are higher for the cells attached to the electrode than it is for the bonds between dividing cells following full completion of septum formation where the firmly attached “mother layer” detaches all its offspring. This makes the whole electrode non-accumulating across time as long as physicochemical conditions remain stable with time then the growth rate will continue depending on the flow rate of feedstock and chemicals and be close as one can get to being a real “true” steady state system.

2.6. Final notes on geometry: scale and size

Marked differences between large volume scale and small scale MFC systems include the surface area to volume ratio (SA:V) of the anodic chamber that increases with smaller volumes. At large scale the fraction of total living cells within the anodic chamber in planktonic suspension is similar in number to the population of active cells attached to the electrode. The smaller the MFC, the less the proportion of planktonic cells there is in the anodic chamber, compared to cells attached to the electrode, at any time. The planktonic contribution towards “side reactions” (e.g. methanogenesis) becomes less important as the anode chamber decreases in size. In small MFC, (<20 ml) the biofilm population outnumbers the planktonic numbers by 10-100-fold, depending on the degree of miniaturisation. The dilution rate of large scale MFC is either zero (i.e. run in batch mode) or low [96], generally below 0.2 h^{-1} and this results in low growth rate and slow metabolic rate and sluggish performance of the biofilm, which is far from its potential optimum. The small degree of hydrodynamic shear is insufficient to shear away daughter cells, thus ending with a thick (diffusion-limited) biofilm. In the presence of excess carbon-energy, large amounts of EPS also contribute to increasing diffusion limitation and slowing metabolic activity and power production. Thick biofilm formation is more likely for large electrode blocks or plates that are impermeable to hydraulic perfusion flow [97]. Highly perfusible electrodes used in combination

with small scale volumes and moderate hydraulic rate may ensure that the biofilm remains free of diffusion limitation throughout its lifetime. However, despite the higher power density at smaller scale, the absolute power output is still relatively small and insufficient to power anything but the smallest of low power devices, so in order to scale up, a multiplicity of MFC units are required [4]. Like batteries, there are two principle ways of connecting a plurality of MFC; in parallel or in series [4]. The advantages of small scale MFC in multiplicity is that each of the units (for example 24 units) is more dynamic than (say) four large volume units where both comparatives have equal total anodic volumes. This means that as well as the collective of 24 having more total power, they will also have a higher collective rate of wastewater treatment ability, since higher power infers faster metabolic rates and therefore faster rates of all bio-transformations.

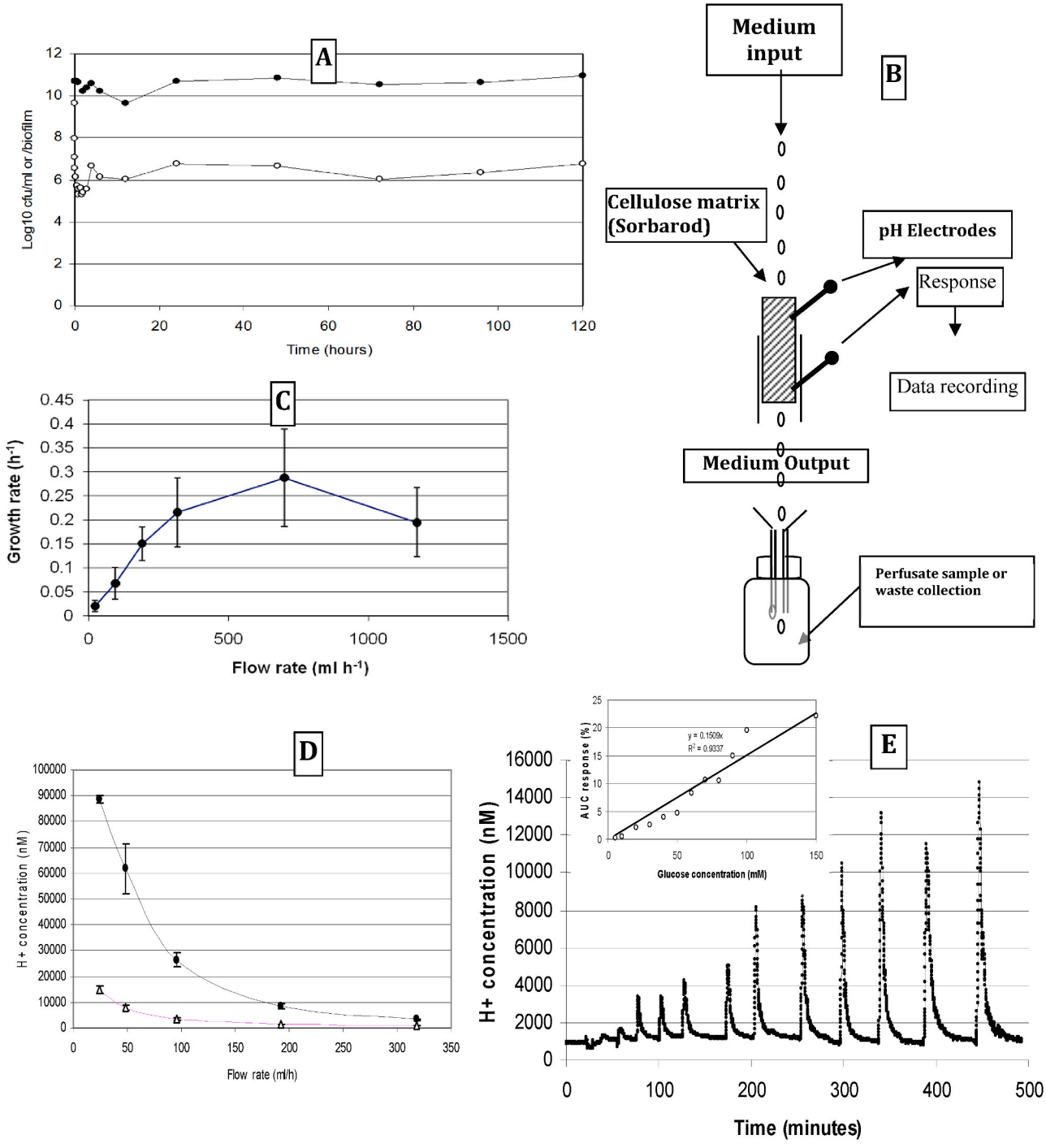

Fig. 8. Biofilm, perfusate populations and rates of glycolysis from the Sorbarod model over time. **A**. Growth of *S. mutans* biofilm perfused with 1/5th strength TYE followed over 3 days. Closed symbols show total biofilm populations; Open symbols show perfusate numbers (cfu ml^{-1}). **B**. Schematic of the Sorbarod perfusion biofilm system with electrodes. **C**. Shows how growth rates (h^{-1}) vary across increasing flow rates (ml h^{-1}); maximum specific growth rate = 0.28 h^{-1}. **D**. Outputs from pH electrodes placed at the top (inflow; open symbol) and bottom (outflow; closed symbol) showing changes in H^+ production with flow rate. The difference between the lines indicates that the pH gradient becomes less the faster the medium is supplied. Therefore, gradients diminish. **E**. Response of model to glucose pulses showing repeated responses to increasing concentration of glucose injected as 0.5 ml pulses. Note the stability of the baseline throughout the experiment. The inset shows the dose response curve.

3. Empirical demonstration of steady state stability

3.1. Non-electroactive species in perfusion biofilms

Studies of biofilm growth rates and their relationship to biofilm thickness have been studied previously [98] but using impermeable substrata (hydroxyapatite). Scientists workers found that the growth profile of the biofilms were similar to the growth profile of the same species grown in planktonic mode. The resemblance in growth rates between planktonic and biofilm bacteria were attributed to the thin and non-dense biofilm formed in the initial stages of the biofilm formation. The thin biofilm coat, reaching a maximal depth of 11 μm, only imposed limited diffusion restrictions, thus did not affect the growth of the bacteria in the biofilm. Their study showed that the growth rate of bacteria on surfaces may resemble their growth in suspension if the bacteria are not embedded in a thick dense biofilm. Perfusion biofilms have been described including Sorbarod-systems [65,70,99,100] that utilise a highly permeable cellulose matrix (the Sorbarod) as an attachment substratum to bind living bacterial cells whilst serving the maximum number of cells with nutrients by advective transport to the cell by setting the speed of the fluidic input and the supply rate of limiting nutrient. The operator can control the rate of growth by controlling the rate of medium in-flow in a similar manner to a chemostat. Such a Sorbarod system [69] was used with *Streptococcus mutans* and the pH monitored by microelectrodes placed at the top and bottom of the biofilm. A Sorbarod was assembled as cylindrical paper sleeve encasing compacted cellulose fibres within a Sorbarod system (Fig. 8B) and inserted into the top of the silicon tubing, where the open ended Sorbarod holder was connected to the collection vessel. Fig. 8A shows the population numbers of cells from the time of inoculation up to 72 h. Growth occurs for both biofilm and perfusate samples over the first 3 h, which then show a decrease followed by an increase before both populations become steady by 6 h followed by a slight reduction between 12 and 24 hours. A schematic diagram of the setup is shown in Fig. 8B whilst Fig. 8C shows how the growth rate varies with the flow rate. The growth rate was thought to be close to maximum at a dilution rate of 0.28 h^{-1}. When fed with dilute TYE without glucose the pH remained relatively constant. However, when biofilms were fed with TYE + glucose (0.2% w/v) a pH gradient occurred when measured from top (input of medium) to bottom (egress of medium) (Fig. 8D). This demonstrates that when glucose was present in the medium at 0.2% (w/v) a marked pH gradient was produced at low steady state flow rates, diminishing at higher steady state flow rates. In general the Sorbarod biofilms continued in a stable manner for up to 14 days when experiments (studying the effects of anti-glycolytic agents) were completed. Fig. 8E shows the effects of injecting pulses of glucose into the system. Note the rapid responses as well as the flat baseline, showing a rapid return to baseline following perturbations. The inset shows the constructed dose response curve. The series of experiments shows the dynamic characteristics of perfusion biofilms. However, the results do indicate that the columnar shape of the Sorbarod coupled with the laminar flow of the medium can produce pH gradients down the matrix indicating a less than perfect homogeneity of the cells. This aspect can be mitigated against by using medium without glucose, or well buffered medium, or a smaller non-tubular, flat-bed matrix model such as that described by Thorn and Greenman [66]. The growth rate of the biofilm at high flow rates ($\mu = 0.28\ h^{-1}$) is many times faster than the growth rates reported for cells in thick diffusion-limiting biofilms, and closer to the value observed for planktonic cells using a chemostat culture for the same respective strain and media [69].

3.2. Electroactive species in perfusion electrode biofilms

A perfect dynamic steady state with regard to any microbial cultures is of course only a theoretical construction whereby all fixed cells are imagined growing at constant rate in response to a constant supply of nutrients and where all other physicochemical factors are constant. The possibility of precisely controlling the growth rate and physicochemical parameters within the anodic chamber of an MFC in a similar way to that achieved in a chemostat was first proposed by Greenman et al. [101]. This paper described a steady state microbial biofilm based on *Geobacter sulfurreducens*. The carbon veil anode electrode acted as the biofilm substratum as well as main end-terminal electron acceptor. The electrical output allowed for the development of the biofilm to be monitored in real time by recording the outputs. The experimental biofilm units were shown to produce constant steady-state current and power output readings over an experimental period of 1 month. Fig. 9 shows a 5 h section of this work. As expected, a change in the resistor load value resulted in a new steady state at a different level of electrical output than the original, yet this output went back to the original levels when the resistance value was changed back. In addition, the transition times between steady states were relatively rapid (around 2–4 minutes). New steady states were also formed by switching streams of substrate although the transition times between steady states were now of longer duration (~ 4–5 minutes) and flow-rate dependent with faster flow resulting in shorter transitional states. The steady-states and the transitional behaviour between the steady-states appeared to be consistent and reproducible. Unfortunately, the levels of perfused cells leaving the system were not monitored. However, this oversight was rectified in a later work [71] where it was shown using viable counts that the specific growth rate of the bacterial biofilms inside an MFC can be controlled. It is also shown that under C/E-limiting conditions, maximum specific growth rate (μ_{max}) coincided with maximum power production, with μ_{max} ($= 0.82\ h^{-1}$) considerably higher than previously thought possible for biofilms. As implied by the authors, both high growth rates and high-power outputs are possible providing that the attachment matrix can allow for homogeneous perfusion of fresh nutrient medium to all cells [63]. It has been suggested that knowing the growth kinetics of *S. oneidensis* MR-1 is essential to fully explore its potential in MFC [102]; this is clearly validated here, calling for similar studies for other anodophile species, with other MFC designs, under "thick" and "thin" biofilm conditions using both C/E excess and C/E-limitation experiments so that MFCs can be optimised in order to maximise both power and transformation of all mineral elements into new biomass and/or carbon dioxide through respiration and creating the power is the cell metabolic reducing power (in the form of NAD(P)H), which is ultimately used to transfer electrons on to the electrode by each cell on a monolayer.

3.3. Diverse mixed cultures and perfusion electrodes

Fig. 10A shows the development of power production in an MFC fed with neat human urine from start-up inoculation (day 1) through the colonisation-biofilm growth phase until maturity (around day 24) followed by steady state until day 45. The anode for this type of MFC was made of soft sponge (15 × 15 × 15 mm) made from polyurethane that had been dipped and coated with a layer of activated carbon; the current collector was made of stainless-steel mesh and Ni–Cr wire was used to connect it to the circuit. The experiment was carried out using continuous-flow, ceramic MFC fed with urine. The MFC was built from cylindrical earthenware membrane supplied with graphite-coated air cathode with internal volume of 11.4 ml. The MFC was prepared as described previously by Pasternak et al. [103]. Note that on day 35 to day 38 the resistance load on the circuit was disconnected, putting the MFC into open circuit mode. This was scheduled in order to measure the recovery time upon re-loading. The connection-disconnection was repeated on day 43. In both cases the recovery was very rapid (within an hour) suggesting that the biofilm had remained stable throughout these periods. Polarisation experiments were also conducted throughout, shown by arrows on Fig. 10A. Fig. 10B shows the type and size of the anode electrode being tested. Fig. 10C shows the results of four of the polarisation experiments indicating that the biofilm was still maturing from day 12 to day 18 but had reached full maturity by day 26.

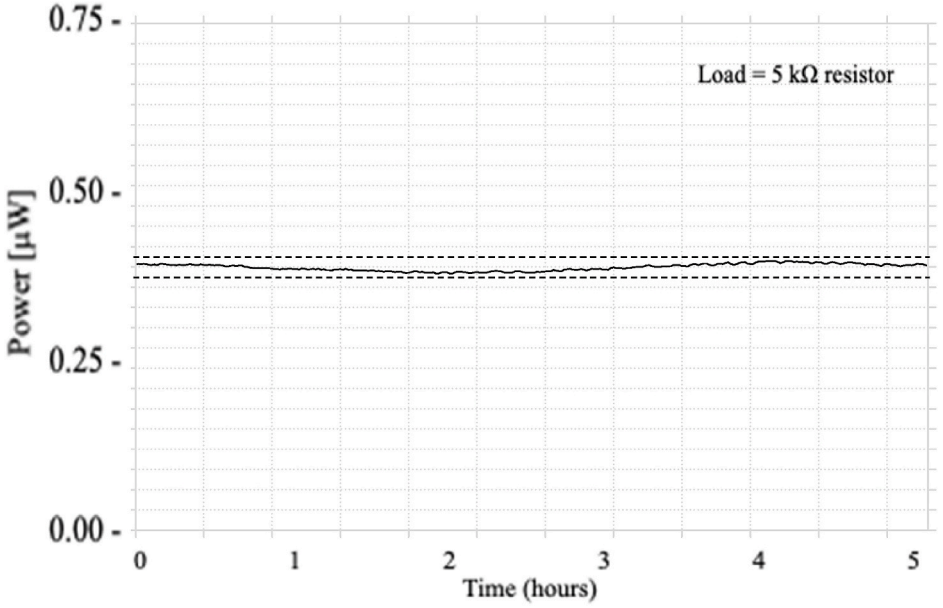

Fig. 9. Steady state power output from Geobacter sulfurreducens. The slight changes in output (<4%) are probably due to slight temperature fluctuations. Reproduced from Greenman et al. [101] with permission from the Publisher.

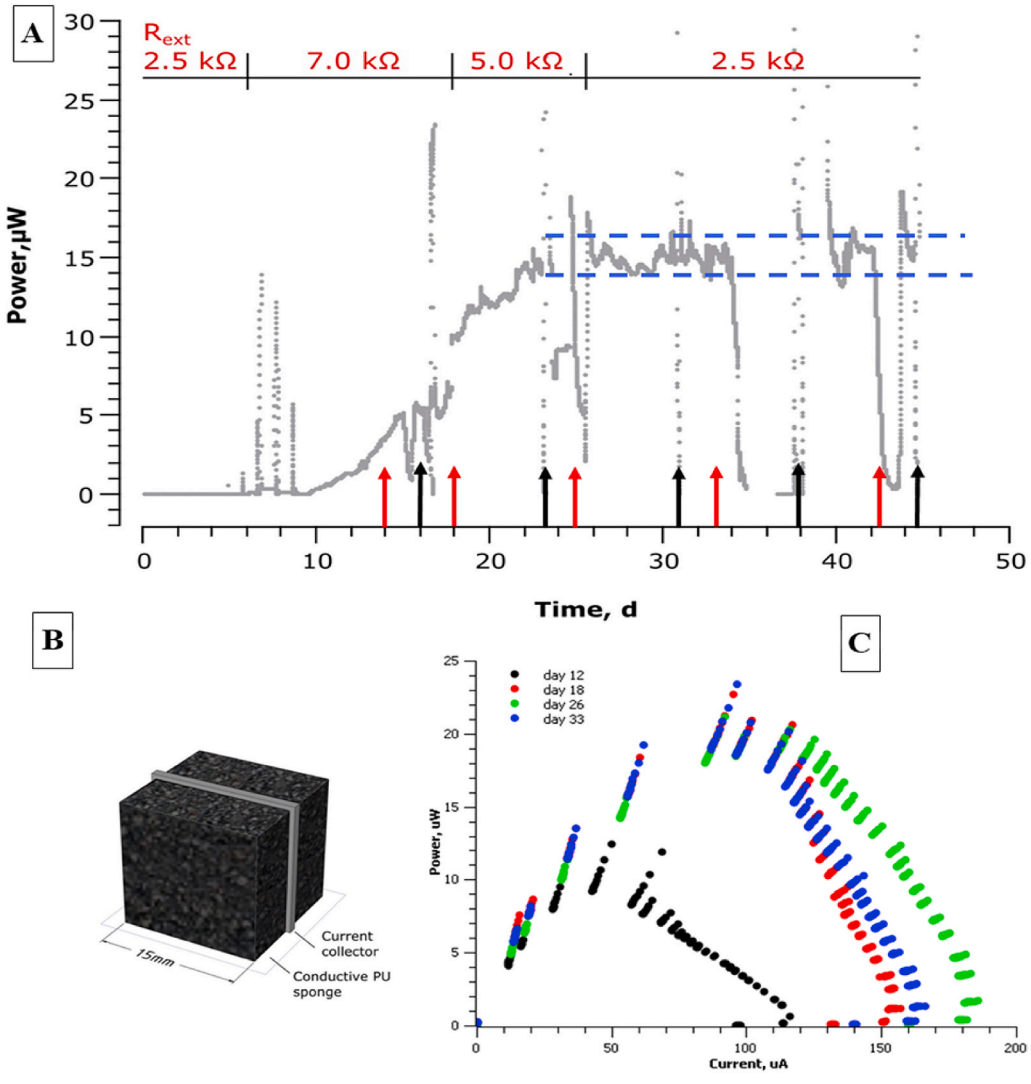

Fig. 10. Experiment to test a carbon coated polyurethane sponge as the anode in small scale MFC. **A**) Temporal MFC output from the start of the experiment. Black arrows show periods when the resistor was disconnected in order to measure the open circuit voltages. Red arrows show periods of time when polarisation experiments were being conducted. **B**) the scheme of the MFC anode used, **C**) power curves performed on 12,18, 26 and 36 day of the experiment. (For interpretation of the references to colour in this figure legend, the reader is referred to the Web version of this article.)

Polarisation data allows the researcher to construct two types of curves (polarisation curves and power curves). A polarisation curve shows the working voltage of the MFC as a function of the current or the current density whilst a power curve presents the power as a function of the current or current density [104]. The power density curve (Fig. 10C) shows the results of four of the polarisation experiments, indicating that the biofilm was still maturing from day 12 to day 18 but had reached full maturity and highest power by day 26. Power curves are very useful for determining the point of maximum power transfer in MFCs. The maximum achievable power (MAP) occurs at the highest power value (where the external resistance is equivalent to the total internal resistance of the cell).

In the above experiment the displacement volume was of 16.3 ml, while the flow rate was equal to 5 mL/h. The population of microbes passing into the MFC from fresh human urine was small ($<10^4$ cells per ml) compared to the active population growing as a biofilm within the carbon coated sponge, which was likely to be in the order of 10^{10}-10^{12} cells in total. On the reasonable assumption that the rate of supply of nutrients was insufficient for the biofilm cells to reach μ_{max} an approximate growth rate (μ) can be estimated to be 0.31 h^{-1}, since the dilution rate = f/V, and in steady state at less than μ_{max} the growth rate equals the dilution rate.

In a different study of the long-term stability of experimental open-to-air cathodes [105] showed that the cathodes, which comprised of two graphite-painted layers separated by a current collector, deteriorated over time due to biofouling of the outer layer. In terms of power output, the initial performance of the MFCs reached average values of 105.5 ± 32.2 μW. After 3 months of operation the power performance decreased to 9.8 ± 3.5 μW and polarisation studies revealed significant transport losses accompanied by biofilm formation on the cathodes. An alkaline lysis procedure was established to remove the biomass and chemical compounds adsorbed on to the cathode's surface. As a result, the power performance of the MFCs recovered to the original level reaching 105.3 ± 16.3 μW, corresponding to a 100% recovery. In addition to showing that the biofilm that formed on the cathode could be successfully removed *in situ* the data also presented strong circumstantial evidence that the performance potential of the anodic electrode biofilm had not significantly changed throughout.

3.4. Experiments on mixed communities

The anodic communities of microbial fuel cell (MFC) are diverse and are made up of different organisms with different functionalities. Nevertheless, the presence, composition and distribution of anodophiles within an MFC is dependent on several factors, including substrate type, inoculation and various reactor parameters [106–109]. A recent study by Obata et al. [110], evaluated the composition and distribution of anodic bacterial community of urine-fed MFC reactors over a 90 day period. The anode was made up of carbon veil while the cathode consists of carbon veil coated with activated carbon. Analysis of the anodic bacterial community observed *Firmicutes* as dominant strains at the earlier stages of the experiment during biofilm establishment (30 days), while in the later stages (60–90 days) the community shifted towards the dominance of *Proteobacteria*, which is important for bioelectrochemical and biochemical reactions related to electrical current generation. Electrochemical performance of both bio-anodes and MFCs could be then related to the shift in bacterial community structure observed after the first 30 days of operation and resulting in redistribution of bacterial strains corresponding to an increase in power generation and establishment of steady-state. During later stages of the experiment (60–90 days) under continuous supply of feedstock and continuous electricity production, the community remained largely stable over time.

Research has shown that different types of microorganism are detected in different MFC systems, which depend on various operational parameters [106,108]. Nevertheless, the choice of anolyte or substrate and its composition is one of the most important factors that determine the structure, and composition of the microbial community of the anode [111]. Urine fed MFC have so far been colonised by certain peculiar types of bacteria that are quite different from the conventional and well known electrogens such as Geobacter and Shewanella. Most of the previously reported bacterial community in urine fed systems were also detected in the current study including Burkholderiaceae, *Tissierella, Pseudomonas*, *Aerococcaceae*, *Atopostipes*, *Peptoniphilus*, *Oligella*, *Proteiniphilum* and *Desulfovibrio* among others [110]. Moreover, the ability of the bacterial community detected within urine-fed MFC systems to generate considerable amounts of current density, which is comparable to other anolytes such as wastewater [112,113], is an indication that there are many more electrogenic bacteria in urine-fed systems that have not been formally identified and characterised. There are indications that these organisms (including *Archaea* that were not determined in this study) possess different metabolic requirements yet operate in a synergistic manner to bring about urine degradation and electricity generation.

It has always been assumed that biofilm-associated organisms grow more slowly than planktonic organisms [114] probably because a majority of cells in the biofilm are limited by nutrient and/or oxygen depletion. This is true of thick diffusion limiting systems but is a misconception if applied to fast (high flow) perfusible systems on anode electrodes where the anode is the sole or main end terminal electron acceptor. Here the opposite situation arises where the biofilm grows more quickly than the planktonic cells.

One possible explanation of how a layer of conductive exoelectrogens can ensure steady state even when diverse species are present is given below in Fig. 11. Growth rate of all species depends on supply rate (flow rate) of limiting nutrients, in particular the organic carbon-energy compounds as the source of electrons. In anaerobic conditions there is no access to oxygen as the end terminal electron acceptor. Nitrate, nitrite, sulphate can be utilised as can carbon dioxide (by methanogens) but in all cases the species that are capable of using these are slow growing. The only species that can grow at high rates are heterotrophic fermenters and the exoelectrogens that can use the anode as the electron acceptor. In contrast to thick biofilms where the highest growth rates are in the outer layers of the biofilm, the fastest growing species in the electrode biofilm are the innermost layers. Both the shedding of cells and mechanical forces are from the core to the outer layers.

Some assumptions to explain stability:

i. Not all biofilms are thick diffusion limited systems with slow growth rates.
ii. The hydrodynamic force required to detach cells (F_{det}) is higher for cells attached to substratum than it is between attached cells and new progeny after full septum formation and division. Liquid shear stress alone could be used to ensure a non-accumulative steady state by using high shear/high flow rates.
iii. Non-electrogenic biofilms forming on perfusible substrata at moderate to high flow rates can be stable for a few weeks until they become thick biofilms.
iv. Biofilms containing anodophiles forming on perfusible anodic electrodes (where the electrode is the sole or main end-terminal electron acceptor) at moderate to high flow rates can be stable for as long as favourable physicochemical conditions allow. This could be for years or decades.
v. Progeny cells from monolayer are shed off naturally because (a) they are more hydrophobic and/or (b) they possess natural shedding systems (e.g. BpfG release and activation of proteinase digesting BpfA dispersing biofilm in *Shewanella*).

Consequences:

i. High stability over long periods of time

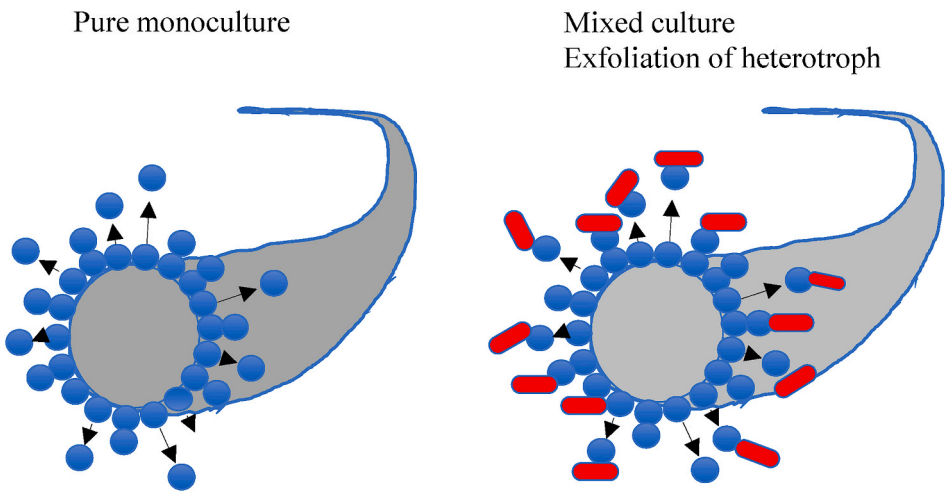

Fig. 11. Exclusion-exfoliation theory for explaining stability. The grey coloured object represents a graphite thread or strand, one of many in carbon veil. The blue particles represent conductive electroactive species. The red particles represent heterotrophic species (typically bacteria that ferment organic substrates). Mixed culture: Inner "core" pushes out any attached heterotrophs that may themselves be dividing. Outer cores are mechanically pushed away by exfoliating daughter cells from the inner core of cells. Heterotrophs adhere to outside surface of daughter cells so wash away as an aggregate of cells and exoelectrogens. The exposed surface "becomes" the next daughter cell and also pushes away. The process repeats. Even though heterotrophs are growing, the vast majority are washed away with the rest. (For interpretation of the references to colour in this figure legend, the reader is referred to the Web version of this article.)

ii. Biofilm reactors can be designed that work a bit like chemostats with external control of physicochemical environment including growth rate by controlling growth-limiting substrate supply rate.
iii. Such biofilm reactors would not be fiercely selective for mutations that increase growth rate or affinity for limiting substrate. Such mutations may still occur but will not be selected for (see below).

Attachment and occupancy of a binding site upon a fixed substratum, which has access to flowing nutrients, gives the species in question an important evolutionary advantage over all other species that cannot attach (or whose binding is weak or non-specific or exhibits slow binding kinetics). There may be fierce competition, but this will be for binding and occupancy in the first instance. Once colonisation has occurred then the types of mutations that are commonly encountered in planktonic chemostat systems may still occur but will not be selected for. In a chemostat, mutations spontaneously occur that give rise to either higher affinity (lower Ks) or higher growth rate (μ_{max}), and these in turn lead to population replacement or takeover [115]. But a mutation of the same type will have little advantage in a biofilm system since all mutant progeny are washed away and unable to accumulate. Only if a mutant arose that could (a) bind stronger than the attached occupant (b) lyse, hydrolyse or otherwise remove or eject the current occupant to take its place (c) subvert the natural dissemination process in biofilms (the washing away of new progeny); only then would the mutant have a selective advantage and dominate. Hence biofilm reactors will be more stable than planktonic chemostats. The same arguments can be applied to takeover by any potentially contaminating immigrant species and may explain the exclusion of pathogens in MFC's treating urine [116].

3.5. Diverse mixed culture MFC biofilms; dilution rate and power

Work by You et al. [117] showed the effects of increasing the flow rate of C/E limited feedstock on power output from a small scale (30 ml chamber volume) MFC with an open-to-air cathode. The biofilm was developed from a mixed highly diverse culture derived from sewage sludge. Following inoculation and one week of batch replacement of feedstock, the system was set to continuous flow using synthetic wastewater as the feedstock, starting at a flow rate of 19.2 ml h^{-1}. Sodium acetate was used as the carbon energy source at variable concentrations, ranging between 0.1 mM and 4.0 mM. Throughout the work, a 1.5 kW external load was connected to each MFC, the value of which was determined based on polarisation runs. All experiments were carried out in a temperature-controlled environment, at 22° C, and repeated at least 3 times. The flow rate (and thus the dilution rate) was varied across the range from 19.2 ml h^{-1} ($D = 0.576\ h^{-1}$) up to 307 ml h^{-1} ($D = 10.2\ h^{-1}$) allowing for steady state between each change.

The work showed that there was an optimum distance of 1 cm between the anode and the membrane for maximum power output. The maximum tested dilution rate ($D = 10.2\ h^{-1}$) was thought to be quite high, yet there was no observable detrimental effect of liquid shear rate causing cell detachment or reduction of electrical output, which suggests that the biofilms on the electrode were very strongly attached and resilient to shear force removal. Furthermore, using an acetate concentration of 2 mM acetate it was shown that the flow rate had a large effect on power outputs (showing that supply rate was just as important as concentration). A K_s value (the half-rate saturation constant) was calculated to be 1.114 mM.

For a chemostat, $\mu = D$. Assuming the MFC biofilm bioreactor behaves like a chemostat then all points below $D \sim 2.5\ h^{-1}$ the dilution rate is insufficient to establish saturation, (i.e. the flattening parts of the graph – Fig. 12), where further increases of flow rate/dilution rate have no further effects. At $\mu = D = 1.5\ h^{-1}$ it can be seen that the saturation point is not quite reached, so μ_{max} will lie somewhere between these two values, we estimate $\sim 2.0\ h^{-1}$ (about 20 minutes doubling time). This gives a mean generation times of minutes rather than hours, shorter than generally thought possible for an environmental biofilm and are as fast as the majority of fast-growing heterotrophic species in chemostats. The rates are 10–20 times faster for μ than those assumed or measured or reported for thick biofilms [118,119].

Mixed bacteria usually produce higher power densities in MFCs than pure bacterial strains, but no single species can be directly compared with another, unless all environmental parameters are identical; yet identical parameters means that some species may be close to their optimum, whilst others would be sub-optimum. From the literature it is obvious that MFC (whatever scale employed) are capable of utilising an enormous range of pure or mixed substrates including aliphatic and aromatic compounds, from monomers to polymers. A list would probably include carboxylic acids (acetate, propionate, butyrate), hydroxylcarboxylic acids (lactate, glycolate, pyruvate, acetoacetate), alcohols (methanol, ethanol, propanol, glycerol), aldehydes, (methanal, ethanal, propanal), ketones (propanone, butanone, pentan-3-one), esters, amides, nitriles, amines, amino acids, alkanes and alkenes. This would also include the sugars, glucose, sucrose, lactose, ribose and deoxyribose nucleotides and nucleosides. With regard to aromatic compounds, then the list would include arenes (benzene and methylbenzene), aryl halides (e.g. chlorobenzene), phenol, phenylamine (aniline) and diazonium compounds. With regards to polymeric compounds then the list would include polysaccharides (including starch, cellulose, chitin, pectin, lignocellulose and lignin), di-peptides, tri-peptides, oligopeptides, proteins, lipids, triglycerides, phospholipids, RNA and DNA.

It is generally thought that the best inocula to use for experiments are

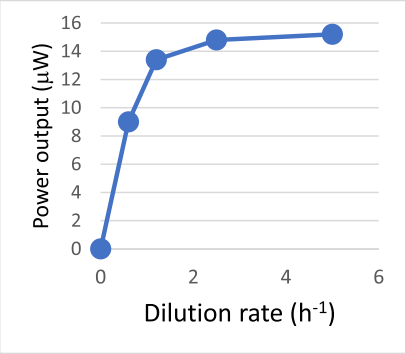

In steady state, $\mu = D$

Doubling time = $\ln 2/\mu = 0.693/\mu$

For $\mu = 1.5$, the doubling time = 0.462h = 28 minutes
For $\mu = 2.0$, the doubling time = 0.346h = 20 minutes
For $\mu = 2.5$, the doubling time = 0.277h = 17 minutes

Fig. 12. Power output versus dilution rate. Data taken from previous work, parts of which have been published in You et al. [117].

obtained from microcosms already adapted to grow on a particular target substrate by species enrichment. Some of the most obvious waste streams to treat are complex mixes of different substrate classes, such as sewage sludge [120], urine [121], brewery waste [122] and wastes that are polluted by heavy metals, examples including landfill leachate [123] but MFC appear to work in a satisfactory manner when supplied with almost anything organic, including petroleum hydrocarbons [124] and would probably utilise some of the many types of plastic materials [125, 126] providing these are supplied in suitable form (e.g. as microplastic spheres). Microbial strains have now been isolated that are capable of breaking down a wide range of long or short chain polymeric substrates.

It follows that in a steady state anodic biofilm system there is a direct relationship between population number of adherent cells and electrical power output (P) is proportional to "N" (biofilm population number of active cells). However, cell quantity alone is not the only governing factor since if all cells are dead with zero metabolic rate there would be zero power, so it is clear that the cells' metabolic rate (Q_{met}) is the most important feature, which is directly proportional to power: $P \propto Q_{met}$. In continuous flow, in steady state the power output and metabolic rate relates to the cells' growth rate (μ) [127].

$P \propto Q_{met} \propto \mu$

The main assumptions for the above to hold true are that:

i. The anode electrode is the only end terminal electron acceptor of significance in the chamber (levels of oxygen, sulphate and nitrate are low or non-existent).
ii. The mixing of substrate into the biofilm is ideal, and the substrate gradient within a thin perfusible biofilm is neglected.
iii. The substrate concentration change from input to output and the supply rate are the main parameters affecting the biofilm growth rate and power output.
iv. The temperature remains constant, and the pH is kept constant via buffering or pH controller (pH auxostat) or medium composition where cells produce acid and base in equal measure.
v. The main overpotential affecting the cathode potential is the activation loss. For simplification and because of the small changes in the cathode open circuit potential (OCP), the cathode OCP is assumed to be constant.
vi. There is no further addition of active biomass to the biofilm. Cells that detach from the anodic biofilm are devoid of an end-terminal electron acceptor so become relatively inert and wash out at a rate depending on the flow rate, the liquid shear stress and the affinity of attachment of the cell to the electrode surface.

We have found that small scale MFC have practical advantages over large scale MFC fermenters where the anodic volume is greater than about 50–100 ml. Large fermenters are built for dealing with large volumes in a single large unit (e.g. 1 m^3) usually in batch culture. The larger the unit, the more likely there will only be one or two replicates that can be used, giving low confidence in the data. All experiments should be replicated as should the number of control MFC that are used for comparison. As a tool for carrying out experiment's replication is a prerequisite. In contrast, a matrix of n = 6, 9 or 12 replicated MFC produce more data and improve the quality of statistical data regarding growth rate and metabolic rate. The tool can help with understanding of bacterial physiology and ecology by exposure of electrodes to set changes in substrates, flow rates, pH or temperature. By use of synthetic mixes of substrates and defined mixtures of colonising microorganisms, then the measurements of metabolic rates by power output and cell production rates (by enumeration of cells and/or optical density) should relate in the same way as cells growing in a chemostat. The metabolic theory of ecology (MTE) using an extension of Kleiber's laws on allometric scaling, posits that the growth rate/metabolic rate of organisms is the fundamental biological rate that governs most of the observed patterns in ecology [128]. MTE provides a unified theory for the importance of metabolism in driving pattern and process in biology from the level of cells all the way to the biosphere. The theories will be applicable for use in attempting to extend single MFC into large stacks, particularly for stacks containing cascades of MFC. One theory that should be tested (in the future) would be a law describing the differential dissemination of fastest growing species by setting flow rates beyond those required for μ_{max}.

CRediT authorship contribution statement

John Greenman: Conceptualization, Data curation, Formal analysis, Investigation, Methodology, Visualization, Supervision, Writing – original draft, Writing – review & editing, Funding acquisition. **Iwona Gajda:** Visualization, Writing – review & editing. **Jiseon You:** Investigation, Formal analysis, Writing – review & editing. **Buddhi Arjuna Mendis:** Visualization, Writing – review & editing. **Oluwatosin Obata:** Investigation, Data curation, Formal analysis, Writing – original draft. **Grzegorz Pasternak:** Writing – original draft, Investigation, Formal analysis, Data curation. **Ioannis Ieropoulos:** Conceptualization, Funding acquisition, Project administration, Resources, Supervision, Writing – review & editing.

Declaration of competing interest

The author(s) declare no competing financial interests.

Acknowledgment

The authors would like to thank the Bill and Melinda Gates Foundation, grant numbers OPP1189676, OPP1149065 and INV-006499 for funding this work.

References

[1] Potter MC. Electrical effects accompanying the decomposition of organic compounds. Proc R Soc B Biol Sci 1911;84:260–76. https://doi.org/10.1098/rspb.1911.0073.

[2] Liang P, Duan R, Jiang Y, Zhang X, Qiu Y, Huang X. One-year operation of 1000-L modularized microbial fuel cell for municipal wastewater treatment. Water Res 2018;141:1–8. https://doi.org/10.1016/j.watres.2018.04.066.

[3] Qian F, He Z, Thelen MP, Li Y. A microfluidic microbial fuel cell fabricated by soft lithography. Bioresour Technol 2011;102:5836–40.

[4] Ieropoulos I, Greenman J, Melhuish C. Microbial fuel cells based on carbon veil electrodes: stack configuration and scalability. Int J Energy Res 2008;32:1228–40. https://doi.org/10.1002/er.

[5] Greenman J, Ieropoulos IA. Allometric scaling of microbial fuel cells and stacks: the lifeform case for scale-up. J Power Sources 2017;356:365–70. https://doi.org/10.1016/J.JPOWSOUR.2017.04.033.

[6] Ledezma P, Degrenne N, Bevilacqua P, Buret F, Allard B, Greenman J, et al. Dynamic polarisation reveals differential steady-state stabilisation and capacitive-like behaviour in microbial fuel cells. Sustain Energy Technol Assessments 2014;5:1–6. https://doi.org/10.1016/J.SETA.2013.10.008.

[7] Sackmann EK, Fulton AL, Beebe DJ. The present and future role of microfluidics in biomedical research. Nature 2014;507:181–9. https://doi.org/10.1038/nature13118.

[8] Sonawane JM, Patil SA, Ghosh PC, Adeloju SB. Low-cost stainless-steel wool anodes modified with polyaniline and polypyrrole for high-performance microbial fuel cells. J Power Sources 2018;379:103–14. https://doi.org/10.1016/J.JPOWSOUR.2018.01.001.

[9] Yuan Y, Zhou S, Liu Y, Tang J. Nanostructured macroporous bioanode based on polyaniline-modified natural loofah sponge for high-performance microbial fuel cells. Environ Sci Technol 2013;47:14525–32. https://doi.org/10.1021/es404163g.

[10] Yang Y, Liu T, Liao Q, Ye D, Zhu X, Li J, et al. A three-dimensional nitrogen-doped graphene aerogel-activated carbon composite catalyst that enables low-cost microfluidic microbial fuel cells with superior performance. J Mater Chem A 2016;4:15913–9. https://doi.org/10.1039/c6ta05002f.

[11] Goel S. From waste to watts in micro-devices: review on development of membraned and membraneless microfluidic microbial fuel cell. Appl Mater Today 2018;11:270–9. https://doi.org/10.1016/j.apmt.2018.03.005.

[12] Leong JX, Daud WRW, Ghasemi M, Liew K Ben, Ismail M. Ion exchange membranes as separators in microbial fuel cells for bioenergy conversion: a comprehensive review. Renew Sustain Energy Rev 2013;28:575–87. https://doi.org/10.1016/j.rser.2013.08.052.

[13] Salar-García MJ, Ieropoulos I. Optimisation of the internal structure of ceramic membranes for electricity production in urine-fed microbial fuel cells. J Power Sources 2020;451:227741. https://doi.org/10.1016/J.JPOWSOUR.2020.227741.

[14] Lotrič A, Sekavčnik M, Kuštrin I, Mori M. Life-cycle assessment of hydrogen technologies with the focus on EU critical raw materials and end-of-life strategies. Int J Hydrogen Energy 2021;46:10143–60. https://doi.org/10.1016/j.ijhydene.2020.06.190.

[15] Winfield J, Gajda I, Greenman J, Ieropoulos I. A review into the use of ceramics in microbial fuel cells. Bioresour Technol 2016;215:296–303. https://doi.org/10.1016/j.biortech.2016.03.135.

[16] Dumas C, Mollica a, Féron D, Basséguy R, Etcheverry L, Bergel a. Marine microbial fuel cell: use of stainless steel electrodes as anode and cathode materials. Electrochim Acta 2007;53:468–73. https://doi.org/10.1016/j.electacta.2007.06.069.

[17] Walter XA, Gajda I, Forbes S, Winfield J, Greenman J, Ieropoulos I. Scaling-up of a novel, simplified MFC stack based on a self-stratifying urine column. Biotechnol Biofuels 2016;9:93. https://doi.org/10.1186/s13068-016-0504-3.

[18] Tender LM, Gray Sa, Groveman E, Lowy Da, Kauffman P, Melhado J, et al. The first demonstration of a microbial fuel cell as a viable power supply: powering a meteorological buoy. J Power Sources 2008;179:571–5. https://doi.org/10.1016/j.jpowsour.2007.12.123.

[19] Arias-Thode YM, Hsu L, Anderson G, Babauta J, Fransham R, Obraztsova A, et al. Demonstration of the SeptiStrand benthic microbial fuel cell powering a magnetometer for ship detection. J Power Sources 2017;356:419–29. https://doi.org/10.1016/j.jpowsour.2017.03.045.

[20] Park DH, Zeikus JG. Electricity generation in microbial fuel cells using neutral red as an electronophore. Appl Environ Microbiol 2000;66:1292–7. https://doi.org/10.1128/AEM.66.4.1292-1297.2000.

[21] Logan BE, Regan M. Microbial challenges and fuel cell applications. Environ Sci Technol 2006;40.

[22] Lovley DR. Bug juice: harvesting electricity with microorganisms. Nat Rev Microbiol 2006;4:497–508. https://doi.org/10.1038/NRMICRO1442.

[23] Torres CI, Marcus AK, Lee HS, Parameswaran P, Krajmalnik-Brown R, Rittmann BE. A kinetic perspective on extracellular electron transfer by anode-respiring bacteria. FEMS Microbiol Rev 2010;34:3–17. https://doi.org/10.1111/j.1574-6976.2009.00191.x.

[24] Torres CI, Kato Marcus A, Rittmann BE. Kinetics of consumption of fermentation products by anode-respiring bacteria. 2007.

[25] Debabov VG. Electricity from microorganisms. Mikrobiologiia 2008;77:149–57. https://doi.org/10.1134/S002626170802001X.

[26] Allen RM, Bennetto HP. Microbial fuel-cells - electricity production from carbohydrates. Appl Biochem Biotechnol 1993;39–40:27–40. https://doi.org/10.1007/BF02918975.

[27] Oz M, Lorke DE, Hasan M, Petroianu GA. Cellular and molecular actions of Methylene Blue in the nervous system. Med Res Rev 2011;31:93–117. https://doi.org/10.1002/med.20177.

[28] Arup PS. The reductase test for milk. Analyst 1918;43:20. https://doi.org/10.1039/an9184300020.

[29] Shukla AK, Suresh P, Berchmans S, Rajendran A. Biological fuel cells and their applications. Curr Sci 2004;87:455–68.

[30] Babanova S, Hubenova Y, Mitov M. Influence of artificial mediators on yeast-based fuel cell performance. J Biosci Bioeng 2011;112:379–87. https://doi.org/10.1016/J.JBIOSC.2011.06.008.

[31] Habermann W, Pommer EH. Biological fuel cells with sulphide storage capacity. Appl Microbiol Biotechnol 1991;35:128–33. https://doi.org/10.1007/BF00180650.

[32] Marsili E, Baron DB, Shikhare ID, Coursolle D, Gralnick JA, Bond DR. Shewanella secretes flavins that mediate extracellular electron transfer. Proc Natl Acad Sci U S A 2008;105:3968–73. https://doi.org/10.1073/pnas.0710525105.

[33] Rabaey K, Boon N, Höfte M, Verstraete W. Microbial phenazine production enhances electron transfer in biofuel cells. Environ Sci Technol 2005;39:3401–8. https://doi.org/10.1021/es048563o.

[34] Ieropoulos IA, You J, Gajda I, Greenman J. A new method for modulation, control and power boosting in microbial fuel cells. Fuel Cell 2018;18:663–8. https://doi.org/10.1002/fuce.201800009.

[35] Kim B-H, Kim H-J, Hyun M-S, Park D-H. Direct electrode reaction of Fe (III)-reducing bacterium, Shewanella putrefaciens. J Microbiol Biotechnol 1999;9:127–31.

[36] Gorby YA, Yanina S, McLean JS, Rosso KM, Moyles D, Dohnalkova A, et al. Electrically conductive bacterial nanowires produced by Shewanella oneidensis strain MR-1 and other microorganisms. Proc Natl Acad Sci U S A 2006;103:11358–63. https://doi.org/10.1073/pnas.0604517103.

[37] Lovley DR. The microbe electric: conversion of organic matter to electricity. Curr Opin Biotechnol 2008;19:564–71. https://doi.org/10.1016/j.copbio.2008.10.005.

[38] Malvankar NS, Vargas M, Nevin KP, Franks AE, Leang C, Kim B-C, et al. Tunable metallic-like conductivity in microbial nanowire networks. Nat Nanotechnol 2011;6:573–9.

[39] Yang Y, Kong G, Chen X, Lian Y, Liu W, Xu M. Electricity generation by Shewanella decolorationis S12 without cytochrome c. Front Microbiol 2017;8. https://doi.org/10.3389/FMICB.2017.01115.

[40] Wrighton KC, Thrash JC, Melnyk R a, Bigi JP, Byrne-Bailey KG, Remis JP, et al. Evidence for direct electron transfer by a gram-positive bacterium isolated from a microbial fuel cell. Appl Environ Microbiol 2011;77:7633–9. https://doi.org/10.1128/AEM.05365-11.

[41] Kato S, Hashimoto K, Watanabe K. Microbial interspecies electron transfer via electric currents through conductive minerals. Proc Natl Acad Sci U S A 2012;109:10042–6. https://doi.org/10.1073/PNAS.1117592109.

[42] Santoro C, Guilizzoni M, Correa Baena JP, Pasaogullari U, Casalegno A, Li B, et al. The effects of carbon electrode surface properties on bacteria attachment and start up time of microbial fuel cells. Carbon N Y 2014;67:128–39. https://doi.org/10.1016/J.CARBON.2013.09.071.

[43] Champigneux P, Renault-Sentenac C, Bourrier D, Rossi C, Delia M-L, Bergel A. Effect of surface nano/micro-structuring on the early formation of microbial anodes with Geobacter sulfurreducens: experimental and theoretical approaches. Bioelectrochemistry 2018;121:191–200. https://doi.org/10.1016/J.BIOELECHEM.2018.02.005.

[44] Gajda I, Greenman J, Ieropoulos I. Microbial Fuel Cell stack performance enhancement through carbon veil anode modification with activated carbon powder. Appl Energy 2020;262. https://doi.org/10.1016/j.apenergy.2019.114475.

[45] Dobell C. Antony van Leeuwenhoek and his“ little animals.”. New York, NY: Harcourt, Brace and Co.; 1932.

[46] Henrici AT. Studies of freshwater bacteria: I. A direct microscopic technique. J Bacteriol 1933;25:277–87. https://doi.org/10.1128/JB.25.3.277-287.1933.

[47] Zobell CE, Allen EC. The significance of marine bacteria in the fouling of submerged surfaces. J Bacteriol 1935;29:239–51. https://doi.org/10.1128/jb.29.3.239-251.1935.

[48] Heukelekian H, Heller A. Relation between food concentration and surface for bacterial Growth1. J Bacteriol 1940;40:547–58. https://doi.org/10.1128/jb.40.4.547-558.1940.

[49] Jones HC, Roth IL, Sanders WM. Electron microscopic study of a slime layer. J Bacteriol 1969;99:316–25. https://doi.org/10.1128/jb.99.1.316-325.1969.

[50] Characklis WG. Attached microbial growths-II. Frictional resistance due to microbial slimes. Water Res 1973;7:1249–58. https://doi.org/10.1016/0043-1354(73)90002-X.

[51] Costerton JW, Geesey GG, Cheng KJ. How bacteria stick. Sci Am 1978;238:86–95. https://doi.org/10.1038/scientificamerican0178-86.

[52] Mack WN, Mack JP, Ackerson AO. Microbial film development in a trickling filter. Microb Ecol 1975;2:215–26. https://doi.org/10.1007/BF02010441.

[53] Jendresen MD, Glantz PO. Clinical adhesiveness of selected dental materials: an in-vivo study. Acta Odontol Scand 1981;39:39–45. https://doi.org/10.3109/00016358109162257.

[54] Jendresen MD, Glantz PO, Baier RE, Eick JD. Microtopography and clinical adhesiveness of an acid etched tooth surface: an in-vivo study. Acta Odontol Scand 1981;39:47–53. https://doi.org/10.3109/00016358109162258.

[55] McCoy WF, Bryers JD, Robbins J, Costerton JW. Observations of fouling biofilm formation. Can J Microbiol 1981;27:910–7. https://doi.org/10.1139/m81-143.

[56] Coffey BM, Anderson GG. Biofilm formation in the 96-well microtiter plate. In: F A, JL R, editors. Methods mol. Biol., vol. 1149. New York, NY: Humana Press; 2014. p. 631–41. https://doi.org/10.1007/978-1-4939-0473-0_48.

[57] Russell C, Coulter WA. Continuous monitoring of pH and Eh in bacterial plaque grown on a tooth in an artificial mouth. Appl Microbiol 1975;29:141–4.

[58] Coombe R, Tatevossian A, Wimpenny JWT. Bacterial thin films as in vitro models for dental plaque. Surf. Colloid Phenom. Oral Cavity Methodol. Asp. 1981: 239–49. London, U.K.

[59] Peters AC, Wimpenny JWT. A constant-depth laboratory model film fermentor. Biotechnol Bioeng 1988;32:263–70. https://doi.org/10.1002/bit.260320302.

[60] Kharazmi A, Giwercman B, Høiby N. Robbins device in biofilms research. Methods Enzymol 1999;310:207–15. https://doi.org/10.1016/S0076-6879(99)10018-1.

[61] Ceri H, Olson ME, Stremick C, Read RR, Morck D, Buret A. The Calgary Biofilm Device: new technology for rapid determination of antibiotic susceptibilities of bacterial biofilms. J Clin Microbiol 1999;37:1771–6. https://doi.org/10.1128/jcm.37.6.1771-1776.1999.

[62] Helmstetter CE, Cummings DJ. Bacterial synchronisation by selection of cells at division. Proc Natl Acad Sci U S A 1963;50:767–74. https://doi.org/10.1073/pnas.50.4.767.

[63] Gilbert P, Allison DG, Evans DJ, Handley PS, Brown MR. Growth rate control of adherent bacterial populations. Appl Environ Microbiol 1989;55:1308–11.

[64] Gander S, Gilbert P. The development of a small-scale biofilm model suitable for studying the effects of antibiotics on biofilms of gram-negative bacteria. J Antimicrob Chemother 1997;40:329–34. https://doi.org/10.1093/jac/40.3.329.

[65] Hodgson AE, Nelson SM, Brown MRW, Gilbert P. A simple in vitro model for growth control of bacterial biofilms. J Appl Bacteriol 1995;79:87–93. https://doi.org/10.1111/j.1365-2672.1995.tb03128.x.

[66] Thorn RMS, Greenman J. A novel in vitro flat-bed perfusion biofilm model for determining the potential antimicrobial efficacy of topical wound treatments. J Appl Microbiol 2009;107. https://doi.org/10.1111/j.1365-2672.2009.04398.x. 2070–9.

[67] McBain AJ. Chapter 4 in vitro biofilm models. An overview. Adv Appl Microbiol 2009;69:99–132. https://doi.org/10.1016/S0065-2164(09)69004-3.

[68] Slade EA, Thorn RMS, Young A, Reynolds DM. An in vitro collagen perfusion wound biofilm model; with applications for antimicrobial studies and microbial metabolomics. BMC Microbiol 2019;19:1–13. https://doi.org/10.1186/s12866-019-1682-5.

[69] McKenzie C. Perfusion biofilm model to screen compounds for antiglycolysis activity against cariogenic streptococci. Bristol: University of the West of England; 2007.

[70] Spencer P, Greenman J, McKenzie C, Gafan G, Spratt D, Flanagan A. In vitro biofilm model for studying tongue flora and malodour. J Appl Microbiol 2007; 103:985–92. https://doi.org/10.1111/j.1365-2672.2007.03344.x.

[71] Ledezma P, Greenman J, Ieropoulos I. Maximising electricity production by controlling the biofilm specific growth rate in microbial fuel cells. Bioresour Technol 2012;118:615–8. https://doi.org/10.1016/j.biortech.2012.05.054.

[72] Helmstetter CE. A ten-year search for synchronous cells: obstacles, solutions, and practical applications. Front Microbiol 2015;6:1–10. https://doi.org/10.3389/fmicb.2015.00238.

[73] Loeb GI, Neihof RA. Marine conditioning films. Adv Chem 1975;145:319–35. https://doi.org/10.1021/ba-1975-0145.ch016.

[74] Marsh PD, Bradshaw DJ. Dental plaque as a biofilm. J Ind Microbiol 1995;15: 169–75.

[75] van Oss CJ. Chapter three the extended DLVO theory. Interface sci. Technol., vol. 16. Elsevier; 2008. p. 31–48. https://doi.org/10.1016/S1573-4285(08)00203-2.

[76] Bayoudh S, Othmane A, Mora L, Ben Ouada H. Assessing bacterial adhesion using DLVO and XDLVO theories and the jet impingement technique. Colloids Surf B Biointerfaces 2009;73:1–9. https://doi.org/10.1016/j.colsurfb.2009.04.030.

[77] Chong P, Erable B, Bergel A. How bacteria use electric fields to reach surfaces. Biofilms 2021;3:100048. https://doi.org/10.1016/j.bioflm.2021.100048.

[78] Kolenbrander PE, Ganeshkumar N, Cassels FJ, Hughes CV. Coaggregation: specific adherence among human oral plaque bacteria. Faseb J 1993;7:406–13. https://doi.org/10.1096/fasebj.7.5.8462782.

[79] Rickard AH, Leach SA, Hall LS, Buswell CM, High NJ, Handley PS. Phylogenetic relationships and coaggregation ability of freshwater biofilm bacteria. Appl Environ Microbiol 2002;68:3644–50. https://doi.org/10.1128/AEM.68.7.3644-3650.2002.

[80] Stevens MRE, Luo TL, Vornhagen J, Jakubovics NS, Gilsdorf JR, Marrs CF, et al. Coaggregation occurs between microorganisms isolated from different environments. FEMS Microbiol Ecol 2015;91:123. https://doi.org/10.1093/femsec/fiv123.

[81] Donlan RM. Biofilms: microbial life on surfaces. Emerg Infect Dis 2002;8:881–90. https://doi.org/10.3201/eid0809.020063.

[82] Characklis WG. Biofilm processes. In: Characklis WG, Marshall KC, editors. Biofilms. New York: John Wiley & Sons; 1990. p. 195–231. 7.

[83] Brading MG, Jass J, Lappin-Scott HM. Dynamics of bacterial biofilm formation. In: Lappin-Scott HM, Costerton JW, editors. Microb. Biofilms. Cambridge: Cambridge University Press; 2009. p. 46–63. https://doi.org/10.1017/cbo9780511525353.004.

[84] Gilbert P, Evans DJ, Brown MRW. Formation and dispersal of bacterial biofilms in vivo and in situ. J Appl Bacteriol 1993;74:67S–78S. https://doi.org/10.1111/j.1365-2672.1993.tb04343.x.

[85] Gilbert P, Evans DJ, Evans E, Duguid IG, Brown MRW. Surface characteristics and adhesion of Escherichia coli and Staphylococcus epidermidis. J Appl Bacteriol 1991;71:72–7. https://doi.org/10.1111/j.1365-2672.1991.tb04665.x.

[86] Zhang YC, Jiang ZH, Liu Y. Application of electrochemically active bacteria as anodic biocatalyst in microbial fuel cells. Chin J Anal Chem 2015;43:155–63. https://doi.org/10.1016/S1872-2040(15)60800-3.

[87] Ishii S, Suzuki S, Norden-Krichmar TM, Nealson KH, Sekiguchi Y, Gorby YA, et al. Functionally stable and phylogenetically diverse microbial enrichments from microbial fuel cells during wastewater treatment. PLoS One 2012;7:e30495. https://doi.org/10.1371/journal.pone.0030495.

[88] Bond DR, Lovley DR. Electricity production by Geobacter sulfurreducens attached to electrodes. Appl Environ Microbiol 2003;69:1548–55. https://doi.org/10.1128/AEM.69.3.1548-1555.2003.

[89] Read ST, Dutta P, Bond PL, Keller J, Rabaey K. Initial development and structure of biofilms on microbial fuel cell anodes. BMC Microbiol 2010;10:1. https://doi.org/10.1186/1471-2180-10-98.

[90] Sun D, Chen J, Huang H, Liu W, Ye Y, Cheng S. The effect of biofilm thickness on electrochemical activity of Geobacter sulfurreducens. Int J Hydrogen Energy 2016;41:16523–8. https://doi.org/10.1016/J.IJHYDENE.2016.04.163.

[91] Mclean JS, Wanger G, Gorby YA, Wainstein M, Mcquaid J, Ishii SI, et al. Quantification of electron transfer rates to a solid phase electron acceptor through the stages of biofilm formation from single cells to multicellular communities. Environ Sci Technol 2010;44:2721–7. https://doi.org/10.1021/es903043p.

[92] Xiao Y, Zhang E, Zhang J, Dai Y, Yang Z, Christensen HEM, et al. Extracellular polymeric substances are transient media for microbial extracellular electron transfer. Sci Adv 2017;3:1–9. https://doi.org/10.1126/sciadv.1700623.

[93] Pasternak G, Greenman J, Ieropoulos I. Dynamic evolution of anodic biofilm when maturing under different external resistive loads in microbial fuel cells. Electrochemical perspective. J Power Sources 2018;400:392–401. https://doi.org/10.1016/J.JPOWSOUR.2018.08.031.

[94] Thormann KM, Duttler S, Saville RM, Hyodo M, Shukla S, Hayakawa Y, et al. Control of formation and cellular detachment from Shewanella oneidensis MR-1 biofilms by cyclic di-GMP. J Bacteriol 2006;188:2681–91. https://doi.org/10.1128/JB.188.7.2681-2691.2006.

[95] Zhou G, Yuan J, Gao H. Regulation of biofilm formation by BpfA, BpfD, and BpfG in Shewanella oneidensis. Front Microbiol 2015;6:790. https://doi.org/10.3389/fmicb.2015.00790.

[96] Babanova S, Jones J, Phadke S, Lu M, Angulo C, Garcia J, et al. Continuous flow, large-scale, microbial fuel cell system for the sustained treatment of swine waste. Water Environ Res 2020;92:60–72. https://doi.org/10.1002/wer.1183.

[97] Guo K, Prévoteau A, Patil SA, Rabaey K. Engineering electrodes for microbial electrocatalysis. Curr Opin Biotechnol 2015;33:149–56. https://doi.org/10.1016/j.copbio.2015.02.014.

[98] Rozen R, Bachrach G, Zachs B, Steinberg D. Growth rate and biofilm thickness of Streptococcus sobrinus and Streptococcus mutans on hydroxapatite. APMIS 2001; 109:155–60. https://doi.org/10.1034/j.1600-0463.2001.d01-117.x.

[99] Allison D, Maira-Litran T, Gilbert P. Perfused biofilm fermenters. Methods Enzymol 1999;310:232–48. https://doi.org/10.1016/S0076-6879(99)10021-1.

[100] Greenman J, McKenzie C, Saad S, Wiegand B, Zguris JC. Effects of chlorhexidine on a tongue-flora microcosm and VSC production using an in vitro biofilm perfusion model. J Breath Res 2008;2:046005. https://doi.org/10.1088/1752-7155/2/4/046005.

[101] Greenman J, Ieropoulos I, McKenzie C, Melhuish C. Microbial Computing using Geobacter biofilm electrodes: output stability and consistency. Int J Unconv Comput 2006;2:249–65.

[102] Tang YJ, Meadows AL, Keasling JD. A kinetic model describing Shewanella oneidensis MR-1 growth, substrate consumption, and product secretion. Biotechnol Bioeng 2007;96:125–33. https://doi.org/10.1002/bit.21101.

[103] Pasternak G, Greenman J, Ieropoulos I. Regeneration of the power performance of cathodes affected by biofouling. Appl Energy 2016;173:431–7. https://doi.org/10.1016/j.apenergy.2016.04.009.

[104] Logan BE, Hamelers B, Rozendal R, Schröder U, Keller J, Freguia S, et al. Microbial fuel cells: methodology and technology †. Environ Sci Technol 2006;40: 5181–92. https://doi.org/10.1021/es0605016.

[105] Pasternak G, Greenman J, Ieropoulos I. Comprehensive study on ceramic membranes for low-cost microbial fuel cells. ChemSusChem 2016;9:88–96. https://doi.org/10.1002/cssc.201501320.

[106] Chae K-J, Choi M-J, Lee J-W, Kim K-Y, Kim IS. Effect of different substrates on the performance, bacterial diversity, and bacterial viability in microbial fuel cells. Bioresour Technol 2009;100:3518–25. https://doi.org/10.1016/j.biortech.2009.02.065.

[107] Chen J, Hu Y, Zhang L, Huang W, Sun J. Bacterial community shift and improved performance induced by in situ preparing dual graphene modified bioelectrode in microbial fuel cell. Bioresour Technol 2017;238:273–80. https://doi.org/10.1016/j.biortech.2017.04.044.

[108] Park Y, Cho H, Yu J, Min B, Kim HS, Kim BG, et al. Response of microbial community structure to pre-acclimation strategies in microbial fuel cells for domestic wastewater treatment. Bioresour Technol 2017;233:176–83. https://doi.org/10.1016/j.biortech.2017.02.101.

[109] Zhang L, Fu G, Zhang Z. Electricity generation and microbial community in long-running microbial fuel cell for high-salinity mustard tuber wastewater treatment. Bioelectrochemistry 2019;126:20–8. https://doi.org/10.1016/J.BIOELECHEM.2018.11.002.

[110] Obata O, Salar-Garcia MJ, Greenman J, Kurt H, Chandran K, Ieropoulos I. Development of efficient electroactive biofilm in urine-fed microbial fuel cell cascades for bioelectricity generation. J Environ Manag 2020;258:109992. https://doi.org/10.1016/j.jenvman.2019.109992.

[111] Choudhury P, Uday USP, Mahata N, Nath Tiwari O, Narayan Ray R, Kanti Bandyopadhyay T, et al. Performance improvement of microbial fuel cells for

waste water treatment along with value addition: a review on past achievements and recent perspectives. Renew Sustain Energy Rev 2017;79:372–89. https://doi.org/10.1016/j.rser.2017.05.098.

[112] Ge Z, He Z. Long-term performance of a 200 liter modularized microbial fuel cell system treating municipal wastewater: treatment, energy, and cost. Environ Sci Water Res Technol 2016;2:274–81. https://doi.org/10.1039/c6ew00020g.

[113] Zhang Y, Liu M, Zhou M, Yang H, Liang L, Gu T. Microbial fuel cell hybrid systems for wastewater treatment and bioenergy production : synergistic e ff ects , mechanisms and challenges. Renew Sustain Energy Rev 2019;103:13–29. https://doi.org/10.1016/j.rser.2018.12.027.

[114] Donlan RM. Role of biofilms in antimicrobial Resistance : ASAIO journal. Am Soc Artif Intern Organs J 2000;46:S47–52.

[115] Wick LM, Weilenmann H, Egli T. The apparent clock-like evolution of Escherichia coli in glucose-limited chemostats is reproducible at large but not at small population sizes and can be explained with Monod kinetics. Microbiology 2002; 148:2889–902. https://doi.org/10.1099/00221287-148-9-2889.

[116] Ieropoulos I, Obata O, Pasternak G, Greenman J. Fate of three bioluminescent pathogenic bacteria fed through a cascade of urine microbial fuel cells. J Ind Microbiol Biotechnol 2019. https://doi.org/10.1007/s10295-019-02153-x.

[117] You J, Greenman J, Ieropoulos I. Novel analytical microbial fuel cell design for rapid in situ optimisation of dilution rate and substrate supply rate, by flow, volume control and anode placement. Energies 2018;11:2377. https://doi.org/10.3390/en11092377.

[118] Van Loosdrecht MCM, Heijnen SJ. Biofilm bioreactors for waste-water treatment. Trends Biotechnol 1993;11:117–21. https://doi.org/10.1016/0167-7799(93)90085-N.

[119] Valquier-Flynn H, Wilson L, Holmes CE, Wentworth C. Growth rate of Pseudomonas aeruginosa biofilms on slippery butyl methacrylate-Co-ethylene dimethacrylate (BMA-EDMA), glass and polycarbonate surfaces. J Biotechnol Biomater 2017;7. https://doi.org/10.4172/2155-952x.1000274.

[120] Jiang J, Zhao Q, Zhang J, Zhang G, Lee D-J. Electricity generation from bio-treatment of sewage sludge with microbial fuel cell. Bioresour Technol 2009;100:5808–12.

[121] Ieropoulos I, Greenman J, Melhuish C. Urine utilisation by microbial fuel cells; energy fuel for the future. Phys Chem Chem Phys 2012;14:94–8. https://doi.org/10.1039/C1CP23213D.

[122] Angosto JM, Fernández-López JA, Godínez C. Brewery and liquid manure wastewaters as potential feedstocks for microbial fuel cells: a performance study. Environ Technol 2015;36:68–78.

[123] Greenman J, Gálvez A, Giusti L, Ieropoulos I. Electricity from landfill leachate using microbial fuel cells: comparison with a biological aerated filter. Enzym Microb Technol 2009;44:112–9. https://doi.org/10.1016/J.ENZMICTEC.2008.09.012.

[124] Morris JM, Jin S. Feasibility of using microbial fuel cell technology for bioremediation of hydrocarbons in groundwater. J Environ Sci Heal Part A 2007;43:18–23.

[125] Espinosa MJC, Blanco AC, Schmidgall T, Atanasoff-Kardjalieff AK, Kappelmeyer U, Tischler D, et al. Toward biorecycling: isolation of a soil bacterium that grows on a polyurethane oligomer and monomer. Front Microbiol 2020;11:404. https://doi.org/10.3389/fmicb.2020.00404.

[126] Ru J, Huo Y, Yang Y. Microbial degradation and valorization of plastic wastes. Front Microbiol 2020;11.

[127] Ledezma P, Greenman J, Ieropoulos I. MFC-cascade stacks maximise COD reduction and avoid voltage reversal under adverse conditions. Bioresour Technol 2013;134:158–65. https://doi.org/10.1016/J.BIORTECH.2013.01.119.

[128] Brown JH, Gillooly JF, Allen AP, Savage VM, West GB. Toward a metabolic theory of ecology. Ecology 2004;85:1771–89. https://doi.org/10.1890/03-9000. Ecological Society of America.